EXPERIMENTAL AND FINITE ELEMENT ANALYSIS OF ROTARY DRAW TUBE BENDING PROCESS

A THESIS SUBMITTED TO
THE GRADUATE SCHOOL OF NATURAL AND APPLIED SCIENCES
OF
MIDDLE EAST TECHNICAL UNIVERSITY

BY

FATİH DERE

IN PARTIAL FULFILLMENT OF THE REQUIREMENTS
FOR
THE DEGREE OF MASTER OF SCIENCE
IN
MECHANICAL ENGINEERING

FEBRUARY 2014

Approval of the thesis:

EXPERIMENTAL AND FINITE ELEMENT ANALYSIS OF ROTARY DRAW TUBE BENDING PROCESS

submitted by **FATİH DERE** in partial fulfillment of the requirements for the degree of **Master of Science in Mechanical Engineering Department, Middle East Technical University by,**

Prof. Dr. Canan ÖZGEN
Dean, Graduate School of **Natural and Applied Sciences** _____

Prof. Dr. Süha ORAL
Head of Department, **Mechanical Engineering** _____

Prof. Dr. Haluk DARENDELİLER
Supervisor, **Mechanical Engineering Dept., METU** _____

Prof. Dr. S. Kemal İDER
Co-Supervisor, **Mechanical Engineering Dept., Çankaya University** _____

Examining Committee Members:

Prof. Dr. Mustafa İlhan GÖKLER
Mechanical Engineering Dept., METU _____

Prof. Dr. Haluk DARENDELİLER
Mechanical Engineering Dept., METU _____

Prof. Dr. S. Kemal İDER
Mechanical Engineering Dept., Çankaya University _____

Prof. Dr. Can ÇOĞUN
Mechanical Engineering Dept., Çankaya University _____

Prof. Dr. Müfit GÜLGEÇ
Mechatronics Engineering Dept., Çankaya University _____

Date: 07 – 02 - 2014

I hereby declare that all information in this document has been obtained and presented in accordance with academic rules and ethical conduct. I also declare that, as required by these rules and conduct, I have full cited and referenced all material and results that are not original to this work.

Name, Last name : Fatih DERE

Signature :

ABSTRACT

EXPERIMENTAL AND FINITE ELEMENT ANALYSIS OF ROTARY DRAW TUBE BENDING PROCESS

DERE, Fatih

M. S., Department of Mechanical Engineering
Supervisor: Prof. Dr. Haluk DARENDELİLER
Co-Supervisor: Prof. Dr. Kemal İDER

February 2014, 65 pages

Rotary draw bending, which has very good flexibility and easy tooling, is one of the most preferred bending types for tubular profiles. Cross-section distortion and the spring-back phenomena are commonly faced problems in bending processes. Spring-back is the inevitable problem that is to be solved by manufacturer, generally by overbending. For hollow tubes cross-section distortion is another difficulty since using hollow tubes results in higher strain rates and distortions. During the process the thickness of the hollow tube at the inner surface, which is contacting with the die, increases and the thickness of the tube at the outer surface decreases. Wrinkling is another important defect that occurs at the inner surface of the tube in large diameter thin walled tube bendings.

This research compares the experimental results with the finite element analysis of the rotary draw bending process. The aim is to obtain bending characteristics of the two material types, SS304 and St37 and so, to reduce the number of the bending in manufacturing. The main parameters in rotary draw bending process are the bending angle, bend radius, material properties and the geometry of the tube that is to be bent. In this study, to deal with the process, two different materials, three different bending angles and three different tube geometries are used in experiments as well as in finite element analysis. In finite element analysis explicit method is used. It is seen that the experimental results are in good agreement with the numerical results.

Keywords: Cross-Section Distortion, Finite Element Method, Rotary Draw Bending, Spring-back, Tube Bending.

ÖZ

DÖNER ÇEKME İLE BORU BÜKME İŞLEMİNİN DENEYSEL VE SONLU ELEMANLAR ANALİZİ

DERE, Fatih

Yüksek Lisans, Makina Mühendisliği Bölümü
Tez Yöneticisi: Prof. Dr. Haluk DARENDELİLER
Ortak Tez Yöneticisi: Prof. Dr. Kemal İLDER

Şubat 2014, 65 sayfa

Döner çekme ile bükme dairesel profiller için kullanılan en yaygın büküm şeklidir. Kesit alanı deformasyonu ve geri yaylanma büküm sırasındaki en çok karşılaşılan problemlerdir. Geri yaylanma genel olarak üretici tarafından fazla bükme ile çözülen kaçınılmaz bir sorundur. İçi boş dairesel boruların kesit deformasyonları, bu profillerde daha fazla gerinim ve bozulma meydana gelmesi nedeniyle dikkate alınması gereken önemli bir problemdir. Döner çekme ile bükme işlemi sırasında, içi boş dairesel profillerin kalıpla temas eden iç yüzeylerindeki et kalınlığı artarken, dış yüzeydeki et kalınlığı ise azalır. Kırışıklık ise büyük çaplı ve ince cidarlı boruların bükümlerinde iç yüzeylerde oluşan bir problemdir.

Bu araştırmada döner çekme ile bükme işleminin deneysel ve sonlu eleman analizi sonuçları karşılaştırılmıştır. Amaç, iki farklı malzeme tipinin, SS304 ve St37, büküm karakteristiklerini elde edip, istenilen üretimin sağlanabilmesi için yapılacak olan büküm sayısını azaltmaktır. Döner çekme ile bükme işlemindeki ana değişkenler büküm açısı, büküm yarıçapı, büküm yapılacak parçanın malzeme özellikleri ve geometrisidir. Bu çalışmada büküm işlemini ele almak için, deneylerde ve sonlu eleman analizlerinde, iki farklı malzeme, üç farklı büküm açısı ve üç farklı boru geometrisi kullanılmıştır. Sonlu elemanlar analizlerinde ise açık metot kullanılmıştır**.** Deney sonuçları ile sonlu eleman analizleri sonuçlarının ile tutarlı olduğu görülmüştür.

Anahtar Kelimeler: Kesit Alan Deformasyonu, Sonlu Elemanlar Metodu, Döner Çekme ile Bükme, Geri Yaylanma, Boru Bükme.

To My Fiancé

ACKNOWLEDGEMENTS

I am grateful to my thesis supervisor Prof. Dr. Haluk Darendeliler for his guidance, endless support and helpful criticism throughout the progress of my thesis study.

I would like to thank Prof. Dr. Kemal İder for his kind help and support throughout my thesis study.

I also want to thank Prof. Mustafa İlhan Gökler, Prof.Dr. Can Çoğun and Prof.Dr. Müfit Gülgeç for their helpful comments.

The cooperation and friendly support of my colleagues in ASELSAN during my thesis study also deserves to be acknowledged.

Finally, many thanks to colleagues Ayşe Özkaya, Emrah Çamlı, Hasan Yılmaz and İbrahim Onur Doğan for their continuous help and understanding during my thesis study.

I am also grateful to my colleague Murat Halisçelik for his support and help which made a valuable contribution to my thesis.

The completion of this thesis would not have been possible without the support from Deniz Taştan who provided important remarks at various stages of my research and encouragement to finish my thesis.

The special thanks go to my parents Saffet Dere and Meryem Dere for their infinite support, and to my sisters Pervin Dere and Penbe Esra Dere.

TABLE OF CONTENTS

ABSTRACT ..... **v**
ÖZ ..... **vi**
ACKNOWLEDGEMENTS ..... **viii**
TABLE OF CONTENTS ..... **ix**
LIST OF TABLES ..... **xi**
LIST OF FIGURES ..... **xii**
NOMENCLATURE ..... **xiv**
CHAPTERS
1. INTRODUCTION **1**
1.1 Bending Types 1
1.2 Rotary Draw Bending 5
1.3 Defects in Bending Processes 6
1.3.1 Wrinkling 6
1.3.2 Spring-back 7
1.3.3 Fracture 8
1.3.4 Cross Section Distortion 8
1.4 Objectives of the Research 9
1.4.1 Outline of the Thesis 10
2. LITERATURE SURVEY **11**
3. FINITE ELEMENT ANALYSIS **15**
3.1 Finite Element Method 15
3.2 Implicit vs Explicit Method 15
4. EXPERIMENTAL ANALYSIS **17**
4.1 Experimental Setup and Tube Bending Operation 17
4.1.1 Tooling 17
4.1.2 Process Parameters and Process Sequence 20
4.2 Determining the Optimum Seam Position 21
4.2.1 Bending Experiments with Different Tube Seam Positions 23
4.2.2 Results 24
4.3 Tube Bending Experiments 25
4.4 Spring-Back Angles and Cross-Section Distortions 25
5. RESULTS **27**
5.1 Finite Element Model 27
5.2 St37 Steel Tubes 31
5.2.1 Stress and Strain Variations of St37 Steel Tubes 31
5.2.2 Wall Thickness Changes of St37 Steel Tubes 33
5.2.2.1 Wall Thickness 1.2 mm 33
5.2.2.2 Wall Thickness 1.5 mm 34
5.2.2.3 Wall Thickness 2 mm 34
5.2.2.4 Comparison of Wall Thickness Changes 35
5.2.3 Cross Section Distortions of St37 Steel Tubes 36
5.2.3.1 Wall Thickness 1.2 mm 37
5.2.3.2 Wall Thickness 1.5 mm 38
5.2.3.3 Wall Thickness 2 mm 39
5.2.3.4 Comparison of Ovalities 39
5.2.4 Spring-back Angles of St37 Steel Tubes 40
5.2.4.1 Wall Thickness 1.2 mm 41

5.2.4.2 Wall Thickness 1.5 mm 41
5.2.4.3 Wall Thickness 2 mm 42
5.2.4.4 Comparison of Spring-back Angles 43
5.3 Results for SS304 Stainless Steel Tubes 43
5.3.1 Stress and strain Variations of the SS304 Stainless Steel Tubes 43
5.3.2 Wall Thickness Changes of the SS304 Stainless Steel Tubes 45
5.3.2.1 Wall Thickness 1.2 mm 45
5.3.2.2 Wall Thickness 1.5 mm 45
5.3.2.3 Wall Thickness 2.0 mm 46
5.3.2.4 Comparison of Wall Thickness Changes 46
5.3.3 Cross-section Distortion for SS304 Steel Tubes 48
5.3.3.1 Wall Thickness 1.2 mm 48
5.3.3.2 Wall Thickness 1.5 mm 48
5.3.3.3 Wall Thickness 2 mm 50
5.3.3.4 Comparison of the Cross-section Distortions 50
5.3.4 Spring-back Simulations for SS 304 Stainless Steel Tubes 50
5.3.4.1 Wall Thickness 1.2 mm 51
5.3.4.2 Wall Thickness 1.5 mm 52
5.3.4.3 Wall Thickness 2 mm 52
5.3.4.4 Comparison of Spring-back Angles 54
6. CONCLUSIONS 55
6.1 Conclusions 55
6.2 Future Work 56
REFERENCES 57
APPENDICES
A. CODEES FOR PREPARING FINITE ELEMENT MODEL 60
B. CASE STUDY: OBTAINING A BENT TUBE HAVING 90° FINAL TUBE ANGLE 64
C. ANGLE MEASURING DEVICE 65

LIST OF TABLES

TABLES

Table 4-1 Geometric Properties of Bend Die 19
Table 4-2 Properties of Clamp Die 19
Table 4-3 Properties of Pressure Die 20
Table 4-4 Process Parameters 20
Table 4-5 Results for SS304 Tube Bendings at Different Tube Seam Positions 24
Table 4-6 Results for St37 Tube Bendings at Different Tube Seam Positions 24
Table 5-1 Material Properties of St37 Steel and SS304 Stainless Steel 28
Table A-1: Finite Element Model for St37 Tube, R=125 mm and t=2 mm……..60

LIST OF FIGURES

FIGURES

Figure 1-1 Push Bending Process 2
Figure 1-2 Hydroforming Process Sequence 3
Figure 1-3 Geometric setup parameters 3
Figure 1-4 Three-roll Tube Bending 4
Figure 1-5 Stretch Bending Process 4
Figure 1-6 (a) V-bending and (b) Air Bending 4
Figure 1-7 Sketch of a rotary draw bending process 5
Figure 1-8 Wrinkled Tube 6
Figure 1-9 Before and After Spring-back 7
Figure 1-10 Fractured Tube 8
Figure 1-11 (a) Collapse on the extrados (b) Cross-section flattening 9
Figure 4-1 Experimental Set-up for Rotary Draw Bending Operations 18
Figure 4-2 Bend Die 18
Figure 4-3 Clamp Die 19
Figure 4-4 Pressure Die 20
Figure 4-5 Rotary Draw Bending Operation 21
Figure 4-6 Unloading of the Pressure Die and Clamp Die and Initialization of Spring-Back 22
Figure 4-7 Seam of the Tube at the Compression Side 22
Figure 4-8 Seam is placed at the Upper Side 23
Figure 4-9 Bent Tubes Used in Finding the Optimum Seam Position 23
Figure 4-10 Bent Tubes 25
Figure 4-11 A 90˚ Bent SS304 Stainless Steel Tube Cut after Bending Operation 26
Figure 4-12 A 120˚ bent St37 Steel Tube Cut after Bending Operation 26
Figure 5-1 Typical LS-DYNA shell elements 27
Figure 5-2 Finite Element Model of the Rotary Draw Bending Process 29
Figure 5-3 Clearance between Clamp Die and Bend Die Insert in Finite Element Model 29
Figure 5-4 Cross-section of the Tubes 30
Figure 5-5 Tube Bending Simulation with different Bend Angles a) 45°, b) 60°, c) 75°, d) 90°, e) 105°, f) 120° 30
Figure 5-6 Stress Variation for the 90º bent St37 Steel Tube Having 2 mm Wall Thicknesses 31
Figure 5-7 Maximum Stress vs Bend Angle for St37 Tubes 32
Figure 5-8 Maximum Equivalent Plastic Strain vs Bend Angle for St37 Tubes 32
Figure 5-9 Wall Thickness Change vs Bend Angle for St37 Steel Tubes having 1.2 mm Wall Thicknesses 33
Figure 5-10 Wall Thickness Change vs Bend Angle for St37 Steel Tubes having 1.5 mm Wall Thicknesses 34
Figure 5-11 Wall Thickness Change vs Bend Angle for St37 Steel Tubes having 2.0 mm Wall Thicknesses 35
Figure 5-12 Wall Thickness vs Wall Thinning for St37 Tubes 35
Figure 5-13 Wall Thickness vs Wall Thickening for St37 Tubes 36
Figure 5-14 Cutting of the 90˚ Bent Tube from its Half Bend Angle 37
Figure 5-15 Shape of the Cross-section after Bending Operation 37
Figure 5-16 Ovality vs Bend Angle for St37 Steel Tubes having 1.2 mm Wall Thicknesses 38
Figure 5-17 Ovality vs Bend Angle for St37 Steel Tubes having 1.5 mm Wall Thicknesses 38
Figure 5-18 Ovality vs Bend Angle for St37 Steel Tubes having 2.0 mm Wall Thicknesses 39
Figure 5-19 Wall Thickness vs Ovalities for St37 Tubes 40

Figure 5-20 Sample Spring-back Solution of the St37 Tube 40
Figure 5-21 Spring-back Angle vs Bend Angle for St37 Steel Tubes having 1.2 mm Wall Thicknesses 41
Figure 5-22 Spring-back Angle vs Bend Angle for St37 Steel Tubes having 1.5 mm Wall Thicknesses 42
Figure 5-23 Spring-back Angle vs Bend Angle for St37 Steel Tubes having 2.0 mm Wall Thicknesses 42
Figure 5-24 Wall Thickness vs Spring-back for St37 Tubes 43
Figure 5-25 Maximum Stress vs Bend Angle for SS304 Tubes 44
Figure 5-26 Maximum Equivalent Plastic Strain vs Bend Angle for St37 Tubes 44
Figure 5-27 Wall Thickness Change vs Bend Angle for SS304 Tubes having 1.2 mm Wall Thicknesses 45
Figure 5-28 Wall Thickness Change vs Bend Angle for SS304 Tubes having 1.5 mm Wall Thicknesses 46
Figure 5-29 Wall Thickness Change vs Bend Angle for SS304 Tubes having 2.0 mm Wall Thicknesses 47
Figure 5-30 Wall Thickness vs Wall Thickening for SS304 Tubes 47
Figure 5-31 Wall Thickness vs Wall Thinning for SS304 Tubes 48
Figure 5-32 Ovality vs Bend Angle for SS304 Steel Tubes having 1.2 mm Wall Thicknesses 49
Figure 5-33 Ovality vs Bend Angle for SS304 Steel Tubes having 1.5 mm Wall Thicknesses 49
Figure 5-34 Ovality vs Bend Angle for SS304 Steel Tubes having 2.0 mm Wall Thicknesses 50
Figure 5-35 Wall Thickness vs Ovalities for SS304 Tubes 51
Figure 5-36 Spring-back Solution of the SS304 Stainless Steel 1.2 mm Wall Thickness Tube 51
Figure 5-37 Spring-back Angle vs Bend Angle for SS304 Tubes having 1.2 mm Wall Thicknesses 52
Figure 5-38 Spring-back Angle vs Bend Angle for SS304 Tubes having 1.5 mm Wall Thicknesses 53
Figure 5-39 Spring-back Angle vs Bend Angle for SS304 Tubes having 2.0 mm Wall Thicknesses 53
Figure 5-40 Wall Thickness vs Spring-back Angles for SS304 Tubes 54
Figure B-1 Tube Bending for the Case Study 64
Figure C-1 Digital Angle Measuring Device 65

NOMENCLATURE

α	Bend Angle
t	Wall thickness of the tubes
d	Inner Diameter of the Tubes
R	Bend Radius
α_f	Angle of the Tube after Bending Operation
S_α	Spring-back Angle
D	Initial Outer Diameter of the Tube
D_{max}	Maximum Diameter of the Tube after the Bending Operation
D_{min}	Minimum Diameter of the Tube after the Bending Operation
O %	Ovalization Value of the Tube after the Bending Operation

CHAPTER 1

INTRODUCTION

Metal forming processes are very widely applied in industry. They are generally preferred to machining processes concerning financial issues and time requirements. Bending, which is a very well-known metal forming process, has an extensive usage in industry and has many application areas and is used in manufacturing of many units varying from small daily devices to very complicated military products. Bending process has some distinct advantages over other manufacturing techniques so that; it may reduce the weight of the system, it may decrease the number of parts used in a mechanical assembly or it may eliminate the use of welds. Bending can be applied not only for closed sections, like tubular or rectangular profiles, but also for some open sections such as T-beams or I-beams. In all of the bending types, tube bending processes are the most applied ones. Some of the application areas of bent tubes are; producing pipelines, highway signs, some chassis frames etc.

With the developing technology new bending types are developed to fulfill the nowadays manufacturing needs. Hydroforming is the process where mainly the hydraulic pressure is used to form the metal component. In hydroforming, generally the material is bent to a required shape with classical bending methods such as compression bending or rotary draw bending and then hydroforming is performed. With the help of hydraulic pressure, it is achieved that thin walled tubes can be bent at 90 degrees with a negligibly small bend radii [1]. Also there are some very basic bending methods such as stretch bending or V bending which are still applied. Concerning all the bending types, rotary draw bending is the most commonly used one.

In all of the bending type's spring-back and cross section distortion are the two inevitable defects. Cross-section distortion can be minimized or decreased by using mandrel in rotary draw bending or by hydroforming (see part 1.1). However, spring-back is always a big concern in all bending processes. Spring-back mainly depends on bend radius, tube geometry and material properties of the tube. The trial and error method which is used in industry mainly depends on over bending. There are many disadvantages of this method; it depends on operator, it has low efficiency and it has high inaccuracy [2]. In order to eliminate the spring-back, spring-back value must be determined beforehand. Otherwise, many trial and error steps would be needed in order to achieve the desired geometry. Selection of the appropriate bending type depends on the repeatability, quality, desired manufacturing rate and also geometry of the part to be bent.

First to give more detail for bending, some information will be conducted on bending types.

1.1 Bending Types

There are many bending techniques utilized by manufacturers. Some comparatively new methods are open to development like hydroforming, laser tube bending or push bending. Moreover, there exist other bending processes such as compression bending, roll bending, V-bending, edge bending and raw bending which are to be explained in detail.

In push bending the tube is placed in to a system involving a die and a plunger. Then an axial load is applied to push the workpiece in to the already shaped die to give the desired geometry to the part. Figure 1-1 is the schematic representation of the process. The aim is to have more uniform profiles compared to other bending techniques such as roll bending and compression bending.

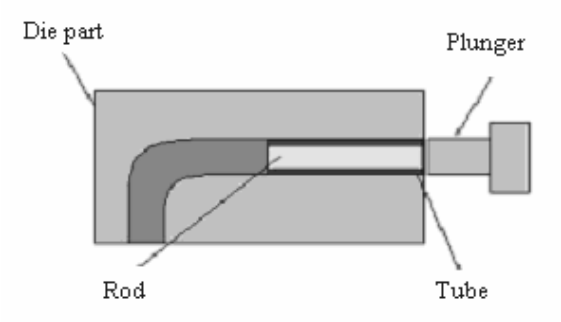

Figure 1-1 Push Bending Process [3]

After pushing the tube and the rod into the die, an internal pressure occurs in the tube by the help of the rod which is flexible. This rod also helps to prevent the wrinkling (see 1.2.6) and serves to reduce the defects. Therefore, the desired bending is achieved with improved characteristics [3].

Compared to other methods like stamping, hydroforming process is relatively new. Research and studies performed on the subject has made the way to generate a state of art of the process. Nevertheless, there is much to investigate on this subject.

Tube hydroforming utilizes fluid pressure to form the materials and it requires expensive equipment for tooling and forming but in hydroforming a variable section part can be obtained effectively. A sample tube hydroforming process sequence is illustrated in Figure 1-2. During the process, after the dies are closed, internal pressure is increased. Axial forces are applied on both sides to make the material flow into the deformation area. Since the inside fluid pressure is same in all contours, a uniform bending profile is obtained [4].

In hydroforming, generally tooling is unique for the desired forming of the material. Therefore the tooling is more expensive compared to other method like rotary draw bending or roll bending.

In hydroforming, selection of the lubricant is crucial since; the lubricant shall have the property to work up to 6000 bars. Furthermore, due to high pressures dies have to be manufactured from steel with certain hardness values. Hydroforming has some drawbacks like slow cycle time, lack of knowledge base and high investment and operational costs. On the contrary, hydroforming has some distinct advantages like, improved structural strength and stiffness, fewer secondary operations, tight dimensional tolerances and lower spring-back values. Taking all these issues into account, feasibility of hydroforming is to be concerned economically and mechanically and compared to conventional techniques before utilizing it [5].

In the last two decades, quite a lot of researches are done on the roll bending processes. The topic is quite popular since tubular profiles and plates can be formed by roll bending, beside plates can be formed to have a conical shape. In roll bending processes geometric setup, positions of the rolls and the position of the workpiece are to be determined properly to satisfy the kinematical relations for reducing the slippage between the rolls and the workpiece. Also, configurations of the rolls affect the surface quality of the bent material.

In Figure 1-3 parameters of a conical roll bending process are shown. Conical rolls are used to satisfy the kinematics, since a conical profile is desired for the workpiece to be bent [6]. To describe a conical profile upper radius, r, lower radius, R, and the height of the conical shape is needed. With those parameters radii of the rolls, R_r, and the distance between the rolls, d, are to be determined.

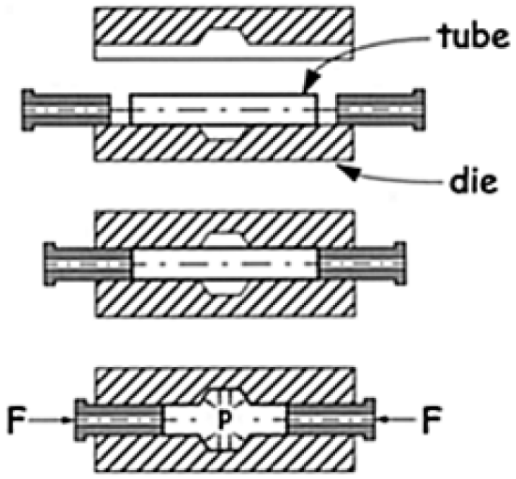

Figure 1-2 Hydroforming Process Sequence [4]

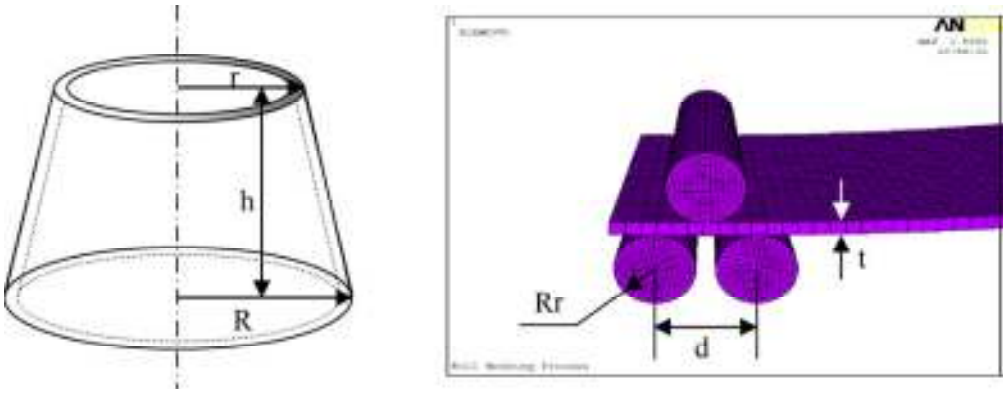

Figure 1-3 Geometric setup parameters [6]

On the other hand, three-roll tube bending is another roll bending type which has an important capability of flexibility. This flexibility comes from the property that only three rolls per tube diameter are needed to obtain any desired bending or geometry.

The three roll bending process setup consists of one or two holding rolls, one bending roll and one setting roll. The motion axes are generally contolled numerically. Three rolls are necessary to achive the bending, but if a more stabilized process is needed, an extra holding roll can be used [7]. A three-roll bending process components are explained in Figure 1-4. An extra holding roll is used in that configuration. The setting roll can be positioned in two axes; it can be rotated around the center o the bending roll (Y-axis) or it can be translated in radial direction (P-axis).

Stretch bending is still being used widely in automotive industry. In stretch bending both ends of the part are under tension. In most of the other methods outer surface is under tension but inner surface is under compression. However, distinctively in stretch bending both surfaces are under tension.

In stretch bending a bending the die is used to give the desired form to workpiece, hydraulic actuators are used to give the tension to workpiece and jaws are used between workpiece and hydraulic actuators to mount the workpiece. As a first step, workpiece is stretched to a chosen value of tension, and after that the fee is given to bending die while the tension is kept constant. Finally, the bending

die finishes its movement and so material is bent [9, 10]. In Figure 1-5 stretch bending process principle is illustrated. Stretch bending is applicable to plates and also tubular profiles.

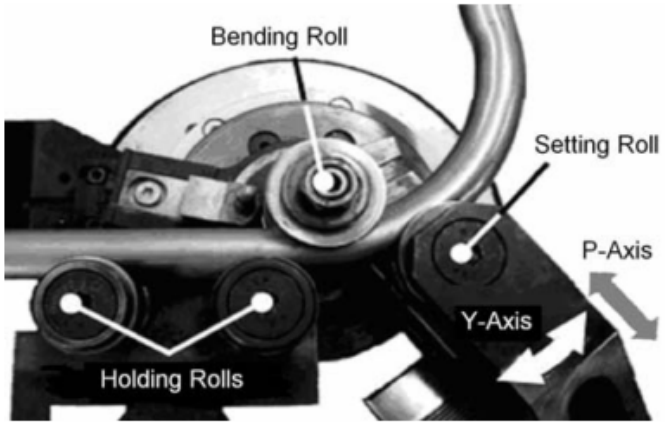

Figure 1-4 Three-roll Tube Bending [8]

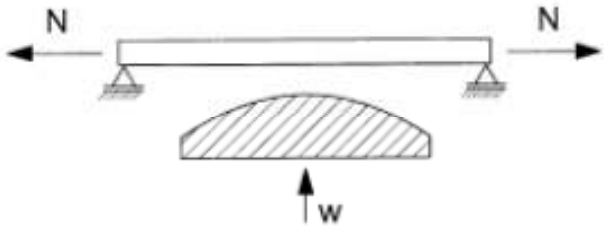

Figure 1-5 Stretch Bending Process [11]

V-bending and air-bending are the two of the most basic bending processes. Air-bending and V-bending are similar processes except one difference; in air-bending the metal is bent in air, but in V-bending metal is formed in a v-shaped die. In both processes a similar ram is fed to the workpiece side to have the desired bending. In Figure 1-6a and Figure 1-6b general principles of V-bending and air-bending are shown respectively.

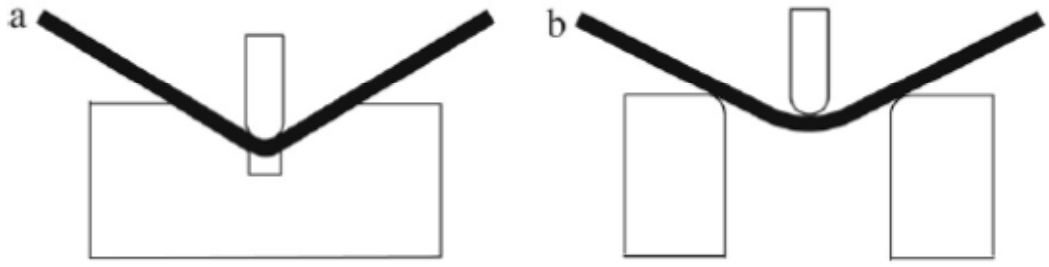

Figure 1-6 (a) V-bending and (b) Air Bending [12]

Air bending serves more flexibility than V-bending, since many bending shapes can be obtained with only one tooling. However, several parameters in air-bending must be considered to avoid precision problems. Among them, spring-back is the hardest phenomenon to control. Spring-back can be minimized using proper tool designs but cannot be eliminated which is same in all bending types [12]. V bending and air bending are applicable to tubular profiles; however, the majority of the manufacturers utilize them for plates. In V-bending there is more contact area between the workpiece and the tools compared to air bending. This can result in less spring-back. However, for thick or heavy materials mass requirements become prohibitive: hence, air bending is used in for thicker profiles [13].

1.2 Rotary Draw Bending

Rotary draw bending is the most commonly used bending process in industry because of its flexibility, cost-effectiveness and high precision. Also, in rotary draw bending higher bending angles can be achieved compared to the other explained bending methods. Not only tubular sections but also other sections like t-beams, rectangular sections, u-beams etc. can be bent with rotary draw bending method. For tubular profiles this process is the most effective and most used bending method.

Tooling mainly consists of bend die, clamp die, pressure die and wiper die. In Figure 1-7 a sketch of a tooling of a rotary draw bending process and a 90 degree bent tube are shown.

Before the process starts, clamp die moves towards the workpiece and so the workpiece is clamped between the bending die and the clamp die on one side. The pressure die is usually fixed but it may also move along with the workpiece. Pressure die may reduce the thinning of the outer section by giving a boost, especially important in high bending angles. After clamping is done properly, bend die starts to rotate with the clamp die synchronously and bending process is completed.

In rotary draw bending process along with the specified tooling a mandrel may be used as well. Mandrel along with wiper die used to prevent wrinkling at the inner side (tool side) of the material. Therefore, mandrel usage is important in thin walled bendings concerning the fact that it prevents the tubes from collapsing.

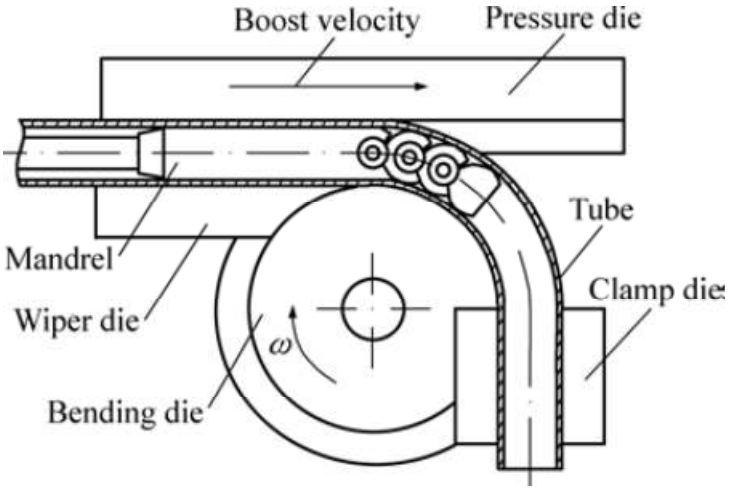

Figure 1-7 Sketch of a rotary draw bending process [14]

Sometimes wiper dies are lubricated before the process to eliminate the drag of the die whereas clamp die and pressure die are used dry in order not to allow slippage between dies and the workpiece.

1.3 Defects in Bending Processes

There are some limitations in bending processes due to defects which occur during bending. Some defects are inevitable but partially controllable whereas some defects are totally unpreventable. Commonly faced defects in bending processes are spring-back, cross-section distortion (or sometimes called as the variation of thickness), wrinkling and fracture.

In some bending applications some defects such as spring-back or cross-section distortion are not very significant. However, in some applications like aerospace industry these defects are needed to be eliminated or at least controlled.

1.3.1 Wrinkling

Thin walled bendings are widely used in mostly automotive and aerospace applications. Because of the trend of using thinner materials having lower weight and higher strength, wrinkling has become one of the most important defects faced in bending processes. Basically, wrinkling is occurring of wavy distortions in the bent surfaces.

In bending if the process parameters such as material thickness or bend radius are chosen improperly, wrinkling can initiate. Wrinkling occurs especially in tubes with large diameter and thin wall thickness. In Figure 1-8 a wrinkled tube having large diameter and thin walls is shown. Solution for this problem is one of the most needed information of bending processes [15].

There are two wrinkling modes in tube bending. First one refers to the local ripples and occurs in straight contours contacting with the die. It is the most observed one. The second one occurs in the bent contours of the material due to slippage of the tube or clamping die. This can be solved by eliminating the slippage. If the system is ensured to have no slippage, only first mode can be considered as the source of wrinkling. Actually, wrinkling is a phenomenon of compressible instability; it occurs in the compressive sides (the inner sides contacting with the bending die) of the tubes due to compressive stresses [15].

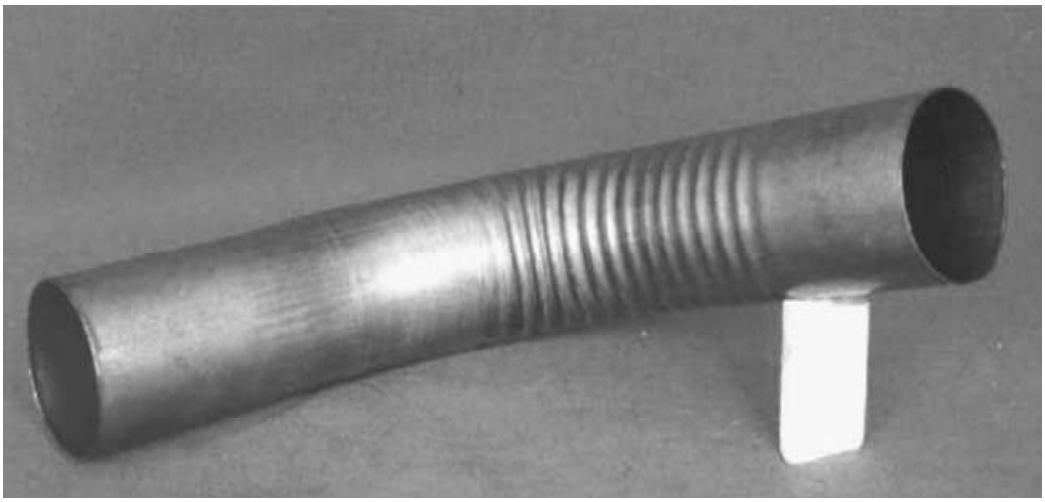

Figure 1-8 Wrinkled Tube [15]

To avoid wrinkling, quite a lot of research is made and wrinkling limit diagrams are generated. A simple wrinkling limit diagram basically shows the minimum bending radius limit for specific tube

geometry in order to avoid wrinkling. Thus, wrinkling is a function of material geometry, material properties, bending type and bending mechanism. It is clear that with using wiper die and mandrel, minimum obtainable bending radius decreases [16].

1.3.2 Spring-back

Spring-back is the most important defect in bending processes. When the material is bent, the inside or the tool side of the workpiece has compressive stresses and the outside of the workpiece has tensile stresses.

After the bending is complete, workpiece is removed from the bending tools. Then, as a result of the elastic properties of the materials, bending angle decreases and bend radii increases after the bending processes. In Figure 1-9, the state which is shown with black dashed lines represents the state before spring-back and the state which is shown with black solid lines represents the state after spring-back of a bent section [17].

It is impossible to have zero spring-back in all of the bending processes. Therefore, spring–back must be taken into account in every bending process. To compensate the spring-back generally higher bend angle and smaller bend radius are used in bending processes to obtain desired dimensions in the final state. On the other hand, variations in the process parameters and material properties affect spring-back dramatically. This means spring-back is always inevitable and difficult to control.

Workpiece continues to spring-back until the bending moment vanishes. Generally, spring-back value depends on material geometry, bend angle, mandrel if used, material properties, tooling and process type (i.e. which bending process used). Also, stress and strain variation is needed since stress balance will be carried out to make a spring-back analysis. In general, spring-back increases linearly with increasing bending angle [18].

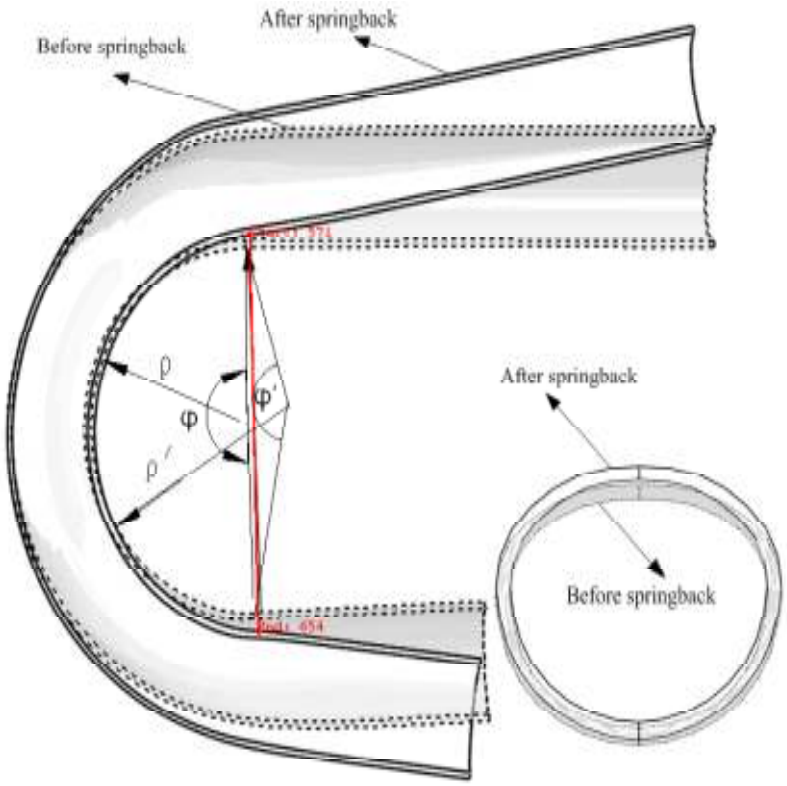

Figure 1-9 Before and After Spring-back [17]

1.3.3 Fracture

Fracture or sometimes it is called bursting is the least seen defect in bending processes. During bending, if the tensile stress in the bending region exceeds ultimate tensile strength of the material, necking starts and after further necking fracture may occur. It is generally faced in bending operation of thin walled structures. In Figure 1-10 an outer surface cracked tube is shown.This defect can be solved by increasing the material thickness, using a higher-strength material or sometimes by reducing the bending angle.

Figure 1-10 Fractured Tube [19]

It is important to note that unexpected fracture have little possibility but still, there may occur sudden, undefined fracture in cases in which highly plastic deformations occur. Even the unpredicted fractures of very well-known materials exist in literature.

1.3.4 Cross Section Distortion

Generally cross-section distortion occurs in two different ways. The section flattens that is shape of the section changes or distorts an also the wall thicknesses changes.

For a tubular section, the cross-sectional deformation profiles are shown on Figure 1-11. In bending of tubular profiles extrados (tube wall at the outer side) gets thinner and intrados (tube wall at the inner section) gets thicker. In Figure 1-11 a cross-section distortion of the bent tube is shown. In Figure 1-11a collapse of the extrados and in Figure 1-11b thinning of the extrados and thickening of the intrados can be recognized.

In industry if the cross-sectional uniformity is important, a developed mandrel or an elastic material is used to provide support from the inside surface of the workpiece for closed sections. With using proper mandrel selection, cross-section distortion can be reduced, but still there will be some distortion at the bent surfaces.

With the new developed hydroforming or push bending technologies cross-section distortion can be controlled more effectively than other bending processes and so flattening of the section and wall thickness changes are minimized. In push bending flexible rod and in hydroforming hydraulic pressure inside the section helps to reduce the defects of bending processes.

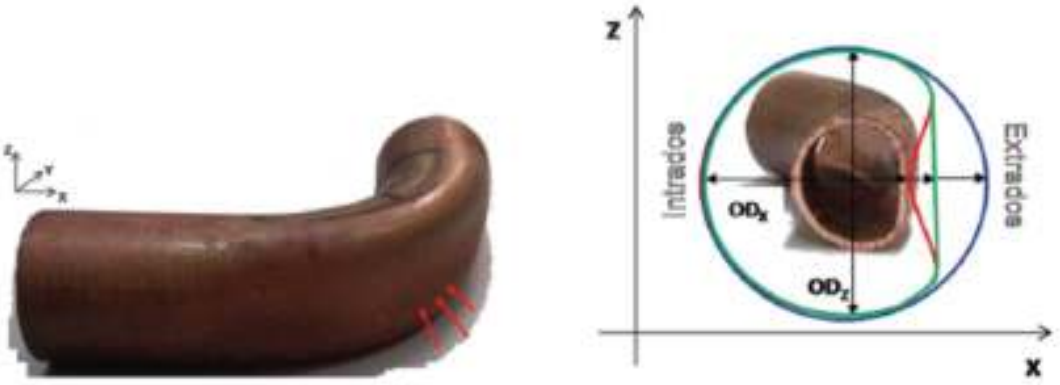

Figure 1-11 (a) Collapse on the extrados (b) Cross-section flattening [20]

1.4 Objectives of the Research

Above, main types of bending processes except rotary draw bending and also defects that are generally faced in bending processes namely; spring-back phenomenon, cross-section distortion, fracture or bursting and wrinkling are described. Rotary draw bending which is the most commonly used bending process is to be explained and analyzed in the present research.

In the next chapter defects are investigated deeply. Literature survey about the defects is presented and analytical model in the literature is discussed. In the finite element analysis chapter a FEM model is generated in the commercial code LS-DYNA.

In the finite element analysis, 2 different material tubes are used namely: SS304 Stainless Steel (or AISI 304) and St37 industry steel. For both materials 3 different tube thicknesses are used. These thicknesses are 1.2, 1.5 and 2.0 mm. Then, for every material and every thickness value 7 different bending angles which are 45º, 60º, 75º, 90º, 105º, 120º and 135º are utilized. By doing so, for both materials 21 different tube bends are performed in finite element analysis. Consequently, 42 different analyses are performed to obtain bending characteristics of the tubes and after that another 42 analyses are performed to obtain spring-back behaviors of the tubes.

In experimental analysis part of the thesis first, 6 tube bends are performed to find the optimum seam position of the steel tube in rotary draw bending operation. After setting the optimum seam position, 18 different tube bending experiments are performed to investigate the wall thickness changes, cross-section distortions and the spring-back angles. In all of the bends same tooling and same rotary draw bending machine is used with 25 mm diameter tubes. The dimensions of the tools and dies are measured and used in finite element analysis part.

After experimental and finite element analysis parts the results are compared and the effects of material properties, bending angle and geometric properties of the tubes on bending defects and stress and strain variations are discussed.

Main goals in this thesis statement are;

i) To perform a parametric study using a commercial code and generate an input code that can be used to investigate different rotary draw bending analysis with different parameters

ii) To find out the optimum seam position for the tubes and then to carry out bending experiments with a rotary draw bending machine used in industry and to obtain spring-

back and cross-section distortion data at the half bend angle in order to come up with suggestions and decrease undesired bendings.

iii) To make use of the generated analysis model to obtain the thickness distribution, cross section distortion and spring-back and also maximum stress and maximum strain variations along the bent tubes.

iv) To compare the results of finite element analysis and experimental analysis to show that the results are in good agreement.

1.4.1 Outline of the Thesis

In this thesis in chapter II, literature search is presented on the work done. In chapter III information is given about finite element method. Chapter IV is the experimental analysis part. In Chapter V the results of the finite element analysis part and experiment part are presented. In the final part conclusions are made and suggestions on the topic are conducted.

CHAPTER 2

LITERATURE SURVEY

In the past many researchers worked on rotary draw bending and investigated its defects as well as the effects of the process parameters. Researchers mainly focused on spring-back, cross section distortion and wrinkling.

Yang, Song, Zhan and Li [17] have worked on spring-back characterization and behaviors of high-strength Ti-3Al-2.5V tubes under cold rotary draw bending. They have studied the effect of loading and unloading procedures for high strength Ti-tubes. The authors divided spring-back into three parts as; significant angular spring-back, radius spring-back and cross sectional spring-back. It is proved that the sectional one decreases the cross-section flattening. They found that both angular and radius spring-back values decrease with the smaller bending radii and the angular spring-back value increases linearly with the increasing bending angle. To deal with the spring-back phenomena they investigated the effects of other process parameters like material kind and material properties and they come up with a two level spring-back compensation method using the finite element simulation results. According to results, smaller Young's modulus results in a larger spring-back angle with larger elastic energy store capacity. Also they noted, higher the strength coefficient, causes larger spring-back. Similarly, higher hardening coefficient n results in a larger spring-back value.

Zhan, Yang and Huang [18] studied spring-back phenomenon to come up with a model to predict spring-back. They put forward a numerical-analytic method for predicting spring-back quickly. They analyzed the spring-back in two steps; obtaining the stress and strain variations and stress balance analysis to predict spring-back. To obtain stress and strain variations they used a rigid-plastic FEM. After that the researchers used an analytic method to perform the spring-back analysis. Besides, authors compared the experiment results and the finite element results. It is found that the maximum relative error is % 17.8 for spring-back angle differences. Moreover, they investigated the effects of strength hardening coefficient and strength hardening exponent on spring-back angles. First a constant strength hardening exponent is taken, and then using different strength hardening coefficients spring-back angle values are investigated. After that, a constant strength hardening coefficient is taken, using different strength hardening exponents spring-back angle values are obtained with respect to the bending angles. They found similar trends with Yang, Song, Zhan and Li's research.

Yang and Lin [15] worked on wrinkling analysis to investigate forming limits for rotary draw tube bending. In the study, a wrinkling wave function is proposed with a wrinkling prediction model. The aim is to obtain minimum bending radius value in order not to have wrinkling, which is also called the wrinkling limit. After that, with the obtained model, they analyzed the effects of tube radius, strength hardening coefficient, strain hardening coefficient and wall thickness on minimum bending radius for tubular profiles in order not to have wrinkling on compressive sides. The authors illustrated that with increasing strain hardening exponent, minimum bending radius decreases. They also found that the minimum bending radius increases almost linearly with increasing strength hardening coefficient of the bent material.

Tang [21] studied plastic-deformation analysis in tube bending and came up with an analytical model to predict seven common unknown tube bending quantities which are stresses, wall thicknesses, shrinking rates at the tube section, deviation of neutral axis, feed preparation lengths of the bend, bending moments and flattening. Pure bending technique is used in the model. The author assumed that the radial stresses in the tube circumferences are negligible since the wall thicknesses of the tubes

are small compared to the tube radii. He started with the basic deformation theory of plastic flow equations came up with some correlations to predict the bending characteristics of tubular profiles.

Agarwal [22] studied analytical and numerical modeling of rotary draw bending process with additional loadings. The aim was to develop a tool that will predict wall thickness variation and cross section distortion accurately. In his study, it is stated that internal pressure or axial pull can be used to achieve better shape control and thickness distribution. He started with the basic plasticity equations and developed an analytical model to see the effects of axial pull and internal pressure on system characteristics. After that, a finite element model is constructed to compare the results with the analytical model, power law plasticity model is used for the Stainless Steel SS304 tubes. Then the results are compared and it is stated that the results are in good agreement. He assumed in his analytical model that the deformation in the rotary draw bending processes is symmetric with respect to the half bend angle sections. Agarwal also tried some combinations of axial pull and internal pressure to have good quality bendings without wrinkling. It is mentioned that with additional loadings wall thickness distribution and cross section distortion can be optimized. With the parametric study performed, he saw that, with an increase in axial pull the rate of decrease in wall thickness was greater at intrados compared to extrados. Moreover, with the analysis done he realized that wrinkling can be prevented with internal pressure alone but the pressure is generally limited with the capacity of pressure intensifier.

Penekli [23] also studied finite element modeling of rotary draw bending process for bending of aluminum profiles. He analyzed tubular, t-beam and u-beam profiles by the finite element method. Some of the results of the finite element analysis are compared with experiments. Penekli also compared his results with other published studies and he stated that the results are in good agreement with those studies. The author stated that maximum total plastic strain decreases as the bend radius increases and also verified that the spring-back angle increases linearly with increasing bend angle. It is also stated that internal pressure acts as a resistant against cross section distortion but internal pressure also increases the strain values especially at the outer sides. Penekli extended his study to see the effects of additional loadings and stated that utilizing stretching force and pressure results in better cross section distortion.

Chunfeng, Yuying, Guofeng, Weili and Junting [24] also stated that with using stretching force in bending, the ratio of elastic deformation to total deformation is decreased, thus spring-back angle is decreased.

Zhao, Liu, Yang, Lu and Gu [25] studied rotary draw bending of 3A21 aluminum alloy rectangular profiles and built a finite element model. A hollow rectangular profile is used in analysis. They used Coulomb friction model on all of the contacting surfaces. After that they compared their results with the experiments performed by Utsum and Sakaki [26] and illustrated that the results are in good agreement with each other. The distribution of tangential stresses has been analyzed. According to the results that Zhao, Liu, Yang, Lu and Gu found, the maximum tangential stress increases sharply in the beginning of the process and then remains nearly constant throughout the bending operation. Basically, circumferential compressive stress regions remain unchanged when the bending process comes to a stable state.

Mentella and Strano [20] had their research on rotary draw bending of copped tubes and mainly focused on cross section distortion. It is stated that maximum deformation and maximum cross-section distortion occurs at the half bend angle of the tubes. They also constructed a simulation model and followed a series of experiments to determine the cross section distortions and they compared the cross-section distortion values of experiments with finite element analysis results. In their research the results were obtained for copper tubes with outer diameter 18 mm and wall thickness 1 mm and the results of the copper tube with outer diameter 16 mm and wall thickness 0.9 mm. The results of finite element analysis and experimental analysis were found close to each other.

Li, Yang, Zhan and Kou [26] also studied deformations of rotary draw bending process. They observed the effects of push assistant loadings and compared the wall thickness changes of bendings with booster and without booster. It is found that for small thickness tubes, booster gets more important concerning the wall thickness changes. They proposed a relation to determine the proper

pressure die length. In their research the results of experiments and simulations are compared for AL-5052O tubes to see the wall thickness change levels. It is stated that maximum effect of push assistant loadings in wall thickness changes was %3. They also realized that the push assistant has more significant effect on the extrados than that on the intrados.

Yang, Jeon and Oh [27] made their research on tube bending of an automotive part. The process was handled in two parts, classical rotary draw bending section as called prebending and hydroforming process. They formed a hollow tie bar having different geometry of cross sections at the end. To perform a proper hydroforming operation, first the workpiece is bent into the desired shape and then in hydroforming sequence with the help of the hydraulic pressure accurate dimensions are obtained and the defects resulting from the prebending section are reduced. The authors first simulated the prebending operation, which is a simple rotary draw bending process and then they used the results of the prebending section to simulate the hydroforming process. The stress and strain distributions are taken as inputs for the hydroforming process. Coulomb friction model is used and anisotropy is not included. In the simulations they found that if the clearance between the wiper die and the tube is important is larger than a certain value, wrinkling appears. It is also stated that when the bending radius is smaller, deformations get higher. They also tried bending with mandrel in prebending section and reached some results. The section shape remained close to circular with the usage of mandrel but the wall thickness change of the tubes was larger.

CHAPTER 3

FINITE ELEMENT ANALYSIS

3.1 Finite Element Method

Finite element tools set light on many engineering problems including many solid mechanics problems. With the developing computer technology, very complicated and highly non-linear problems can be solved numerically. Likewise, finite element method has been used effectively in bending processes simulations. Commercial softwares are available and used effectively in industry and also for academic purposes to simulate many non-linear bending processes.

There are basically two different approaches in solid mechanics problems concerning the order of displacements: small displacement theory and large displacement theory. If the displacements and rotations are small, it is possible to use a linear relationship between strains and displacements. Also in small displacement theory the undeformed and the deformed configurations are the same state. All quantities such as stresses and strains are referred to the original state of the undeformed configuration.

If the small displacement theory is used in a finite element solution, the orders of the strains and rotations shall be considered carefully at the beginning. For the cases of strains and rotations on the order of 10^{-2}, the error resulting from using the small displacement theory is generally less than 1% which is a quite accurate value. It gives better results for the problems having smaller strain and rotation values [28].

In all bending applications there occur very large deformations, therefore large displacement theory shall be applied for all metal forming simulations in order to have accurate results.

In the case of large displacements, the current configuration significantly moves with respect to the initial coordinates. This implies that in numerical analysis every time step large deformations occur. Therefore it is important to identify the reference configuration carefully. There are two different approaches used in engineering problems. In Lagrangian description all quantities are expressed with respect to the initial configuration whereas in Eulerian description all quantities are expressed in terms of the current configuration [28].

Eulerian description is mostly used in fluid mechanics, for solid mechanics Lagrangian description is more suitable. There are also two distinct Lagrangian descriptions used in engineering problems; Total Lagrangian formulation and Updated Lagrangian formulation. In Total Lagrangian formulation all the variables and the equations are introduced with respect to the reference configuration but in the Updated Lagrangian formulation all the variables and the equations are introduced with respect to the current configuration which is identified at the new time step. In many commercial softwares, Updated Lagrangian formulation is used for metal forming applications.

3.2 Implicit vs Explicit Method

The finite element solutions of the solid mechanics, especially non-linear quasi-static problems like bending processes, can be obtained by implicit and explicit method solutions. In both methods the desired solutions are obtained incrementally.

Implicit approach usually has an incremental method having a convergence criterion which is to be satisfied at the end of the solution. The desired solution is obtained when the convergence criteria is satisfied. However, in explicit approach the finite element solution equations are rearranged to make them dynamic and by doing so without any iterations they can be solved incrementally. The solutions at the end of the increments are obtained directly.

Implicit approach is generally used in cases in which time dependency is not a concern. Static problems or structural problems can be analyzed with implicit approach easily. Explicit approach is generally used to solve the cases of large deformations with highly time dependent properties. Crash, impact and metal forming problems are some examples that can be solved effectively by explicit approach. In explicit methods non-linearities can be handled more easily.

Several studies have been published comparing the two approaches. For example; Rebelo et al. [29] realized that implicit approach is more helpful and preferable in basic 2D problems. On the other hand, the explicit approach is more robust for complicated problems. It is very helpful and convenient in problems involving contacts and highly non-linear plasticity.

Time integration is an important issue in explicit dynamic analysis. Many commercial codes use central difference method to update the geometry in the new time step. Also it is found that, in explicit dynamic analysis, more storage is needed to store the displacement vector, however, the results become much less sensitive to round off error [31].

There are also many studies in the literature that are focusing on using the dynamic equations of motion to simulate quasi-static, non-linear processes with finite element method with the implicit approach. It has been an alternative way to use the static, implicit approach in the analysis of solid mechanics problems with plastic deformations. Kutt, Pifko, Nardiello and John [32] studied slow-dynamic simulation of manufacturing processes. They performed a static simulation of a deep drawing process and had accurate results. It is stated that slow-dynamics is competitive approach concerning the accuracy of results and solution times for the non-linear finite element analysis of quasi static problems. With the developing computer hardware technology, the method would be more preferable in future. However, with nowadays technology capabilities utilization of slow dynamic approach for simulating manufacturing processes such as bending deep drawing rolling processes, are only feasible for systems which can be modeled as 2D. Therefore, the method is mainly appropriate for 2D systems in finite element analysis of some manufacturing operations with implicit approach. For 3D systems the slow-dynamic approach is still not preferable concerning the solution times and the accuracy of the results.

Putting all the issues into account, usage of explicit method in finite element simulation of manufacturing processes like rotary draw bending or cold rolling is more appropriate. With explicit method, solution times are reduced, hence, the dynamic system can be modeled in more detail which will give more accurate results in finite element simulations. As a result, in this study, the rotary draw bending operation is analyzed by using explicit finite element method.

CHAPTER 4

EXPERIMENTAL ANALYSIS

In the experimental analysis part, 18 different rotary draw tube bending operations are performed to verify the finite element simulations. The process parameters; length of the pressure die, length of the wiper die, bend radius, tube geometries and tube materials are same with the ones used in finite element analysis part. Besides, 6 bendings are performed before the experiments to find the optimum position of the tube seams in the rotary draw bending processes.

4.1 Experimental Setup and Tube Bending Operation

A numerically controlled rotary draw bending machine has been used to obtain the desired tube bendings. The experiments performed by comparing the spring-back angles, wall thickness changes and the ovalization results. 9 different tube bendings were performed for each material type (SS304 Stainless Steel and St37 Steel). Bending experiment set-up is illustrated in Figure 4-1 and Clamp die, pressure die and the bend die which have been used in the tube bending experiments are labeled.

4.1.1 Tooling

In the experimental set-up, pressure die, clamp die and bend die are utilized for obtaining the rotary draw bending operation. The dies are made of a material with higher strength than the workpiece material in order to prevent the deformation of the dies. Pressure die is produced of a self-lubricant material to provide good slippage between the tube and itself; whereas clamp die and bend die are made of stainless steel.

Bend Die

A stainless steel cylindrically shaped die with a groove on its circumference is manufactured first and then an insert is welded on it to provide the bend die. Outer radius of the bend die sets the bending radius of the process. The insert length is generally taken equal to the clamp die length. The bend die used in the experiments is shown in Figure 4-2 with its insert.

The groove inside the bend die provides a slot for the tubes. Also, accurate manufacturing and proper heat treatment of the bend dies are important since they directly affect the bend radius of the tube bending process. Geometrical properties of the bend die are listed in Table 4-1.

Clamp Die

Clamp die, which has a groove inside, has a similar shape with the bend die insert. The clamping is generally provided with a hydraulic piston which is assembled to the back side of the die. The die that was used in the experiments is shown in Figure 4-3.

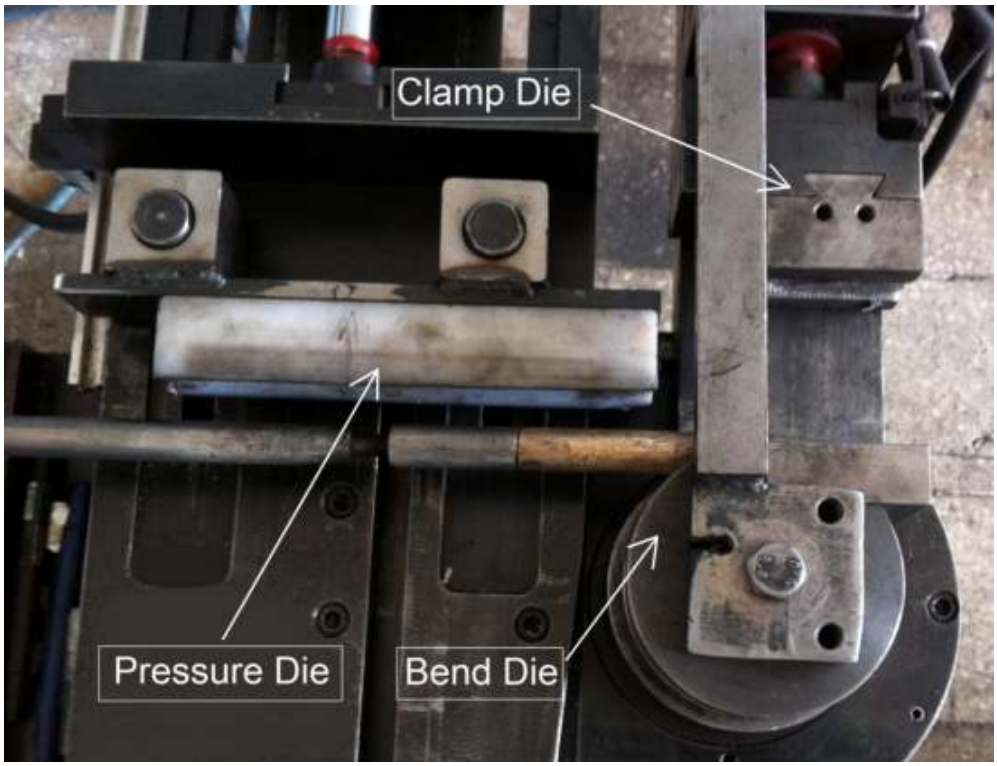

Figure 4-1 Experimental Set-up for Rotary Draw Bending Operations

Figure 4-2 Bend Die

Table 4-1 Geometric Properties of Bend Die

Parameter	**Magnitude**
Length of the Insert	70 mm
Groove Radius	12.5 mm
Outer Radius	62.5 mm

Figure 4-3 Clamp Die

In rotary draw bending processes clamp die is used to hold the tube in position and to prevent slippage. Therefore, there should be enough clamping force to fix one edge of the tube between bend die insert and the clamp die. The clamping force is kept constant during the rotary draw bending process. Properties of the clamp die which was used in the experiments are listed in Table 4-2.

Table 4-2 Properties of Clamp Die

Parameter	**Magnitude**
Length of the die	70 mm
Groove Radius	12.5 mm
Clamping Pressure	160 bar

Pressure Die

Pressure die is made of a self-lubricant material and it is used to keep the unbent material in its position. Pressure die which was used in the experiments is shown in Figure 4-4. In the experiments pressure die was kept stationary. However, in industry boost type pressure dies are also utilized in tube bending operations. In those cases boost speed occurs as a new parameter for the process.

Figure 4-4 Pressure Die

Properties of the pressure die are listed in Table 4-3. Pressure of the pressure die may be increased up to 50 MPa depending on the applications in industry.

4.1.2 Process Parameters and Process Sequence

System parameters related with the dies are given in the tooling section and the other parameters are listed in Table 4-4. Bend angle, material type and tube thicknesses have been selected as variables whereas the other parameters have been kept constant.

Table 4-3 Properties of Pressure Die

Parameter	**Magnitude**
Length of the die	230 mm
Groove Radius	12.5 mm
Pressure Applied	Negligible

Table 4-4 Process Parameters

Parameters	**Magnitude**
Bend Radius	62.5 mm
Outside Diameter of the Tubes	25 mm
Initial Tube Lentghs	1000 mm
Clearance Between the Clamp Die and Bend Die Insert	1.5 mm
Coefficient of Friction Between the Tube and the Pressure Die	0.1
Maximum Bend Radius	180°
Bend Angle	Variable
Tube Thickness	Variable
Materials	SS304, St37

Steps of the rotary draw bending operation,

- Pressure die, clamp die and the rotary bend die are mounted and fixed on the rotary draw bending machine
- Process parameters (bend angle, bend radius, bending time, unloading time etc.) are defined to the rotary draw bending machine via the numerical control window
- Tube is mounted along the bending line (tangent to the bend die)
- The pressure die and the clamp die comes to bending position and fixes the tube
- Bend die rotates around its central axis and the tube is bent
- Dies returns to initial position

Figure 4-5 shows an instant during the tube bending process. The tube is fixed between the bend die and clamp die in order not to allow slippage on the clamped edge of the tube. After the tube is bent, the clamp die is released and the tube spring-backs after unloading. Figure 4-6 illustrates the unloading of a 90º bent tube in rotary draw bending machine.

Figure 4-5 Rotary Draw Bending Operation

4.2 Determining the Optimum Seam Position

The tubes used in the experiments are laser welded. The seam at the inner side of a tube is shown Figure 4-7. The effects of the seam position during the bending process are determined in this section. Also it is aimed to find the proper position for a better quality of bending.

Figure 4-6 Unloading of the Pressure Die and Clamp Die and Initialization of Spring-Back

Figure 4-7 Seam of the Tube at the Compression Side

4.2.1 Bending Experiments with Different Tube Seam Positions

To investigate the effects of the tube seam position on tube bendin,g different seam positions were used for both of the tube materials. The aim is to see the effect of the seam position on the spring-back angle and cross-section distortios and to determine the best seam position for the rotary draw bending process. To achieve this goal, 3 critical tube seam positions are selected: the inner side or the compression side, the upper side and the outer or the tensile side. Noting that the upper and the lower sides are identical considering the rotary draw bending process. In Figure 4-7 the seam is at the compression side and in Figure 4-8 the seam is at the upper side of the tube before the bending operation.

Six different tube bending experiments (3 for the SS304 tubes, 3 for the St37 tubes) were performed. In all of the bendings, bending angle was taken as 90˚ and the thickness of the tubes was 1.5 mm. All bending parameters were kept constant except the material type and seam position. Bent tubes are shown in Figure 4-9.

Figure 4-8 Seam is placed at the Upper Side

Figure 4-9 Bent Tubes Used in Finding the Optimum Seam Position

4.2.2 Results

After completing the bending experiments spring-back angles were calculated as follows;

$$S_\alpha = \alpha - \alpha_f \quad (1)$$

where S_α is the spring-back angle value occurred after unloading, α is the desired bend angle that is defined to the rotary draw bending machine and α_f is the final bend angle after the spring-back occurs. All angle quantities are represented in degrees.

To obtain the maximum cross-section distortion, the tubes were cut from their half bend angle planes to calculate the cross-section distortion values and the distortion values are represented in terms of ovality as given below.

$$O\% = \frac{D_{max} - D_{min}}{D} \times 100 \quad (2)$$

where, D_{max} and D_{max} are maximum and minimum outer diameters and D is the initial outer diameter of the bent tubes respectively [20].

Spring-back and ovality results for the SS304 and St37 tubes are listed in Table 4-5 and Table 4-6, respectively.

Table 4-5 Results for SS304 Tube Bendings at Different Tube Seam Positions

Seam Position	Ovality (%)	Spring-back Angle(°)
Inner Side	10.8	5.0
Upper Side	8.2	4.9
Outer side	11.2	5.1

Table 4-6 Results for St37 Tube Bendings at Different Tube Seam Positions

Seam Position	Ovality (%)	Spring-back Angle(°)
Inner Side	13.3	1.5
Upper Side	10.6	1.5
Outer side	14.3	1.6

Maximum difference in the spring-back angle values were 0.2˚ for SS304 tubes and 0.1˚ for St37 tubes. Results show that the seam position has no significant effect on spring-back angle. However, when the seam was positioned at the compression or the tension side, higher cross-section distortions were observed. Maximum difference in the ovality values was 3.7% for SS304 tubes and 3.0% for SS304 tube bendings for different seam positions. When the seam is positioned at the inner or the outer side, cross-section distortion increases. The minimum cross-section distortion was observed when the seam was positioned at the upper side for both SS304 and St37 tubes.

It is feasible to place the seam at the upper side or the lower side since comparatively much lower stresses occurs. The results obtained for cross-section distortion also imply the same; to achieve minimum ovality values, the seams should be positioned at the upper or the lower side. In the light of the results obtained, the seams have been positioned at the upper side in all of the bending experiments.

4.3 Tube Bending Experiments

In the experiments material type, bend angle and the wall thicknesses were selected as the variables of the process and all other bending parameters had been kept constant throughout the study. Two types of materials were used which are SS304 Stainless Steel, St37 Steel and for each material 3 different tube wall thicknesses were used which are 1.2, 1.5 and 2.0 mm. Also, for each wall thickness, 3 tube bendings were performed with different bend angles which are 60°, 90° and 120°.

In Figure 4-10 all of the bent tubes (9 St37 Steel tubes and 9 SS304 Stainless Steel tubes) are presented. After performing the bending operations, the comparison of the experiment results (i.e. wall thicknesses, spring-back angles and ovalities) and the finite element simulation results were made.

Figure 4-10 Bent Tubes

4.4 Spring-Back Angles and Cross-Section Distortions

After performing the 18 different tube bending operations the bend angles of the tubes were measured and spring-back angles were obtained. Angle measuring device, which has 0.1° measuring sensibility, is shown in Appendix C.

In Figure 4-11, a 1.5 mm wall thickness SS304 Stainless Steel tube and in Figure 4-12, a 1.5 mm wall thickness St37 Steel tube, which were cut from the half bend angle are shown as samples.

Figure 4-11 A 90˚ Bent SS304 Stainless Steel Tube Cut after Bending Operation

Figure 4-12 A 120˚ bent St37 Steel Tube Cut after Bending Operation

After the necessary cross-section cut operations were handled, the ovality measurements and calculations were performed. Besides, maximum and minimum wall thicknesses were measured at intrados and extrados through the cut sections of the bent tubes.

CHAPTER 5

RESULTS

5.1 Finite Element Model

In the finite element models four-noded shell elements were used. Fully integrated shell elements were used to model the tube. Therefore, there is no need for extra hourglass control [30]. Figure 5-1 illustrates the typical shell elements that would be used in finite element modeling of the rotary draw bending processes.

Thickness distributions of the tubes after the bending, spring-back angles, cross-section distortions and maximum total plastic strains were obtained by using the finite element simulations. Results are evaluated for different wall thickness values.

In this thesis pre-processing (model creation, defining the material properties, meshing and identifying the boundary conditions and inertia properties) is performed in ANSYS 11.0. After that the explicit dynamic solver, LS-DYNA is used. For post-processing (plotting the results, obtaining some figures and animating the rotary draw bending system), LSPREPOST is used together with ANSYS 11.0.

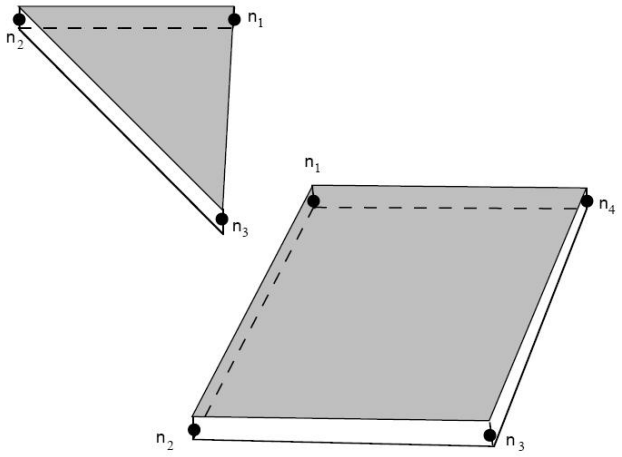

Figure 5-1 Typical LS-DYNA shell elements [30]

In Table 5-1 material properties of St37 Steel and SS304 Stainless Steel tubes are listed.

It is crucial to use proper material model in finite element modeling of solid mechanics problems in which large plastic deformations occur. Power law plasticity model is very widely and effectively used in different metal and plastic forming simulations including bending processes. Elastoplastic behaviour with isotropic hardening is provided with the model. Therefore, power law plasticity model is applied in the current finite element analysis for both material types. In power law plasticity model, the yield stress $\sigma_{y,}$ is a function of plastic strain and satisfies the following equation.

$$\sigma_y = K\varepsilon^n = K(\varepsilon_{yp} + \bar{\varepsilon}^p)^n \quad (3)$$

where ε_{yp} is the elastic strain to yield, $\bar{\varepsilon}^p$ is the effective plastic strain, K is the strain hardening coefficient and n is the strain hardening exponent [31].

Table 5-1 Material Properties of St37 Steel [33] and SS304 Stainless Steel [22]

Material Property	**St37**	**SS304**
Mass density (kg/m^3)	7850	7850
Young's Modulus E (GPa)	207	210
Poisson's Ratio ν	0.28	0.3
Strain hardening coefficient K (MPa)	479.3	1451
Strain hardening exponent n	0.226	0.6
Initial strain ε_0 (mm/mm)	0	0.06

A finer mesh with 4223 shell elements was utilized for the tubes. Mesh profile of pressure die is not so critical; hence, a coarse mesh was used in finite element models with 312 shell elements. To model the bend die and the clamp die 1296 and 592 shell elements were used, respectively. The contacts of the system and frictions are identified to simulate the real life conditions for the bending operation. All dies are defined as rigid bodies. Finally, to simulate the bending operation, the bend die is rotated around its central axis with the desired bend angle to obtain rotary draw bending simulation.

Since wrinkling was not observed in the finite element analysis and bending experiments wiper die was not used in the rotary draw bending system. Also it is clear that it does not have a significant effect on the stress and strain variations and cross-section distortions for the cases performed in the thesis statement.

An input code has been developed which can be used in the commercial code LS-DYNA to obtain rotary draw bending characteristics of the SS304 stainless steel and St37 steel tubes (See Appendix A for a sample code). In the code rotary draw bending system parameters such as bending angle, tube geometrical properties or material model properties were entered. By changing the wall thicknesses, material properties and bend angles, all bending simulations were performed.

Figure 5-2 is an isometric view of the sample finite element model for the rotary draw bending process. Three different tube thicknesses and two different material tubes were used in the experiments and finite element analysis. Since the outer diameter of the tubes were all the same, same tooling was used in all bending simulations and experiments.

The shell element thicknesses and also the gap between the clamp die and bend die insert (given in Table 4-4) were also modeled in finite element analysis as shown in Figure 5-3. Also, all dimensions of the tubes and dies were measured directly from the experimental setup and used in commercial software. The detail for the cross-section of the tubes is illustrated in Figure 5-4, where t is the wall thickness (shell element thickness in the finite element model) and d is the outside diameter of the tubes.

The required tooling dimensions and other needed process parameters to complete the finite element model were used as same with the experiments part (as listed in Table 4-4).

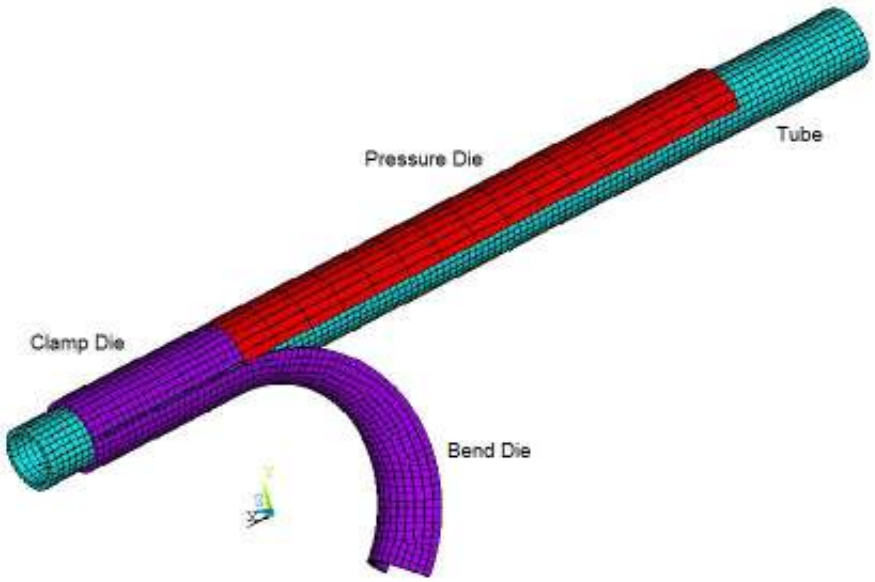

Figure 5-2 Finite Element Model of the Rotary Draw Bending Process

A series of analysis has been performed for rotary draw bending analyses. In the analyses the effects of the variation of the wall thicknesses and the bend angles were concerned. Standard tubular profiles (i.e. standard wall thicknesses and diameters), which are easy to find in the market, were used in the analysis. Finite element analysis results are presented in two parts: rotary draw bending analysis of St37 Steel tubes and rotary draw bending analysis of SS304 Stainless Steel tubes separately. Maximum stress and strain values, wall thickness changes, ovalization values and spring back values of the bend tubes are obtained and presented. Sample tube bending simulations of St37 2.0 mm wall thickness tubes is illustrated in Figure 5-5. 45°, 60°, 75°, 90°, 105° and 120° bent tubes are shown in the figure, respectively.

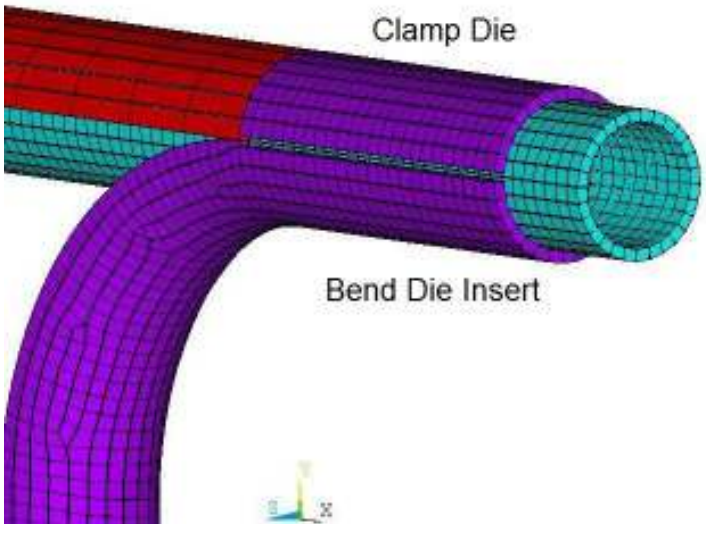

Figure 5-3 Clearance between Clamp Die and Bend Die Insert in Finite Element Model

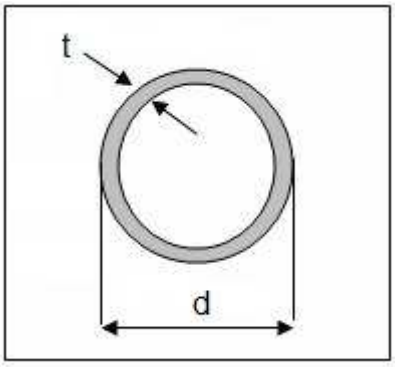

Figure 5-4 Cross-section of the Tubes

Outer radius of the tubes was 25.0 mm. Bend Radius, R, was 62.5 mm. 3 different wall thicknesses were used in simulations for each material, which were 1.2, 1.5 and 2.0 mm. 7 different bend angles were utilized for each wall tube wall thickness of two materials. Bend angles were 45º, 60º, 75º, 90º, 105º, 120º and 135º. Consequently, 21 different explicit analyses were performed for each material type to simulate the rotary draw bending process and so, 42 explicit analyses were conducted in total.

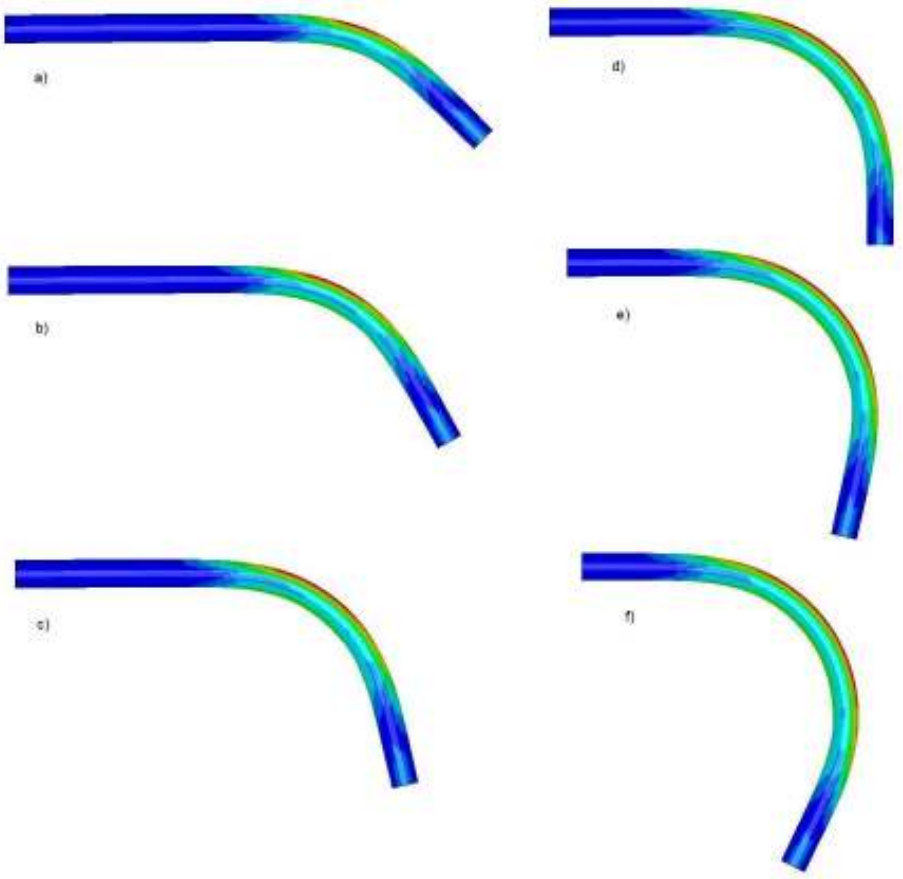

Figure 5-5 Tube Bending Simulation with different Bend Angles a) 45°, b) 60°, c) 75°, d) 90°, e) 105°, f) 120°

5.2 St37 Steel Tubes

Stress and strain variations, wall thickness changes, ovalities and spring-back angles of the St37 tubes are presented in detail and results of the finite element simulations and experiments are compared.

5.2.1 Stress and Strain Variations of St37 Steel Tubes

As an example, stress variation for the 90º bent tube having 2.0 mm wall thickness, is shown in Figure 5-6. Maximum equivalent stress occurs at the outer surfaces of the bent tubes (extrados). Extrados have larger strain values than the inner surfaces (intrados) which are in contact with the bend die.

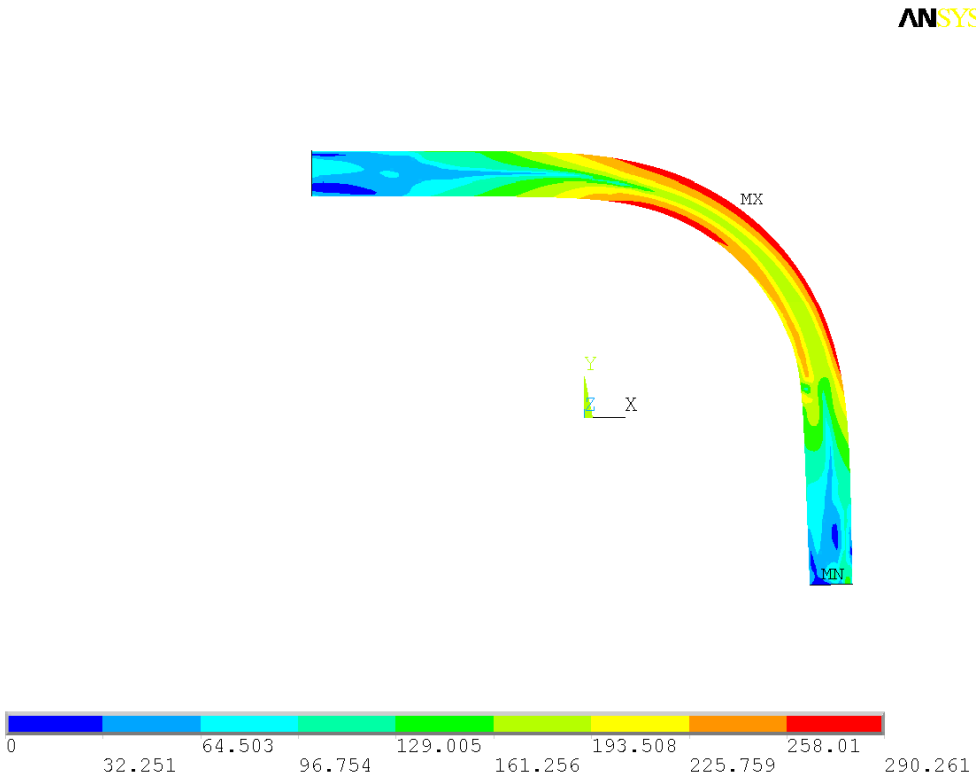

Figure 5-6 Stress Variation for the 90º bent St37 Steel Tube Having 2 mm Wall Thicknesses

Seven different bending simulation results were obtained for each different wall thickness of the St37 Steel tubes. Maximum equivalent stress value for the 2 mm wall thickness tubes has been obtained as 304.8 MPa. Maximum equivalent stresses have been obtained as 321.8 MPa and 338.1 MPa for the 1.5 mm and 1.2 mm wall thickness tubes, respectively. Maximum equivalent stresses at the extrados are plotted in Figure 5-7 including all wall thickness alternatives. The maximum equivalent stresses increase with increasing bending angle.

Large plastic strains were faced in the bending process. The simulations results denote that the wall thickness has an important effect on the strain values. Figure 5-8 was prepared for St37 tubes having different wall thicknesses. For each thickness of the tubes, 7 different maximum equivalent strain values at 7 different bend angles have been included. Maximum equivalent plastic strains for the 1.2 mm, 1.5 mm and 2 mm wall thicknesses were obtained as; 0.238, 0.227 and 0.206, respectively at 135° bending operations. The figure shows that equivalent strains increase with increasing bend angle also it is clear that thicker tubes undergo less strains. Maximum strain and maximum stress values

were encountered in the 135º bending operation since the tube deforms more with increasing bend angle.

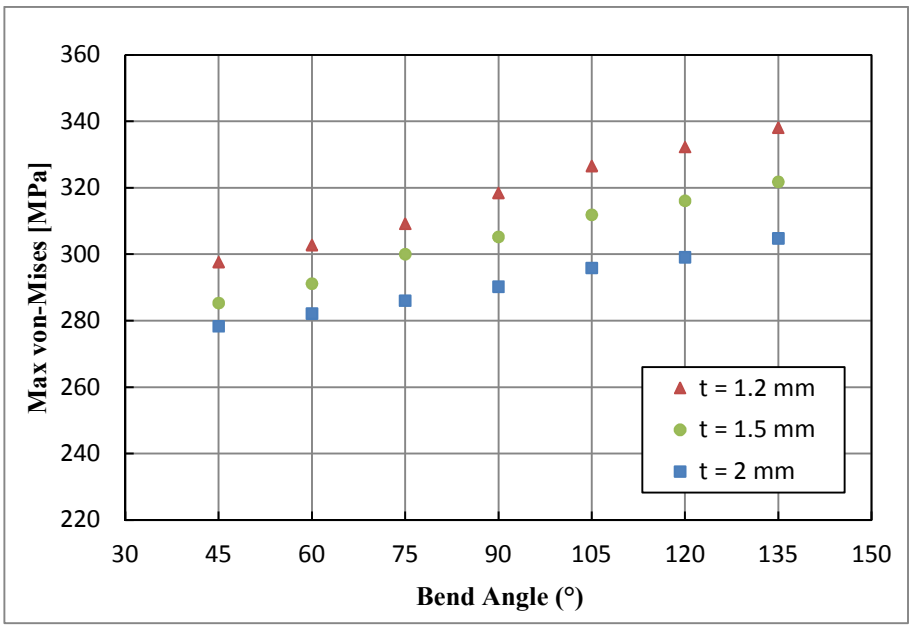

Figure 5-7 Maximum Stress vs Bend Angle for St37 Tubes

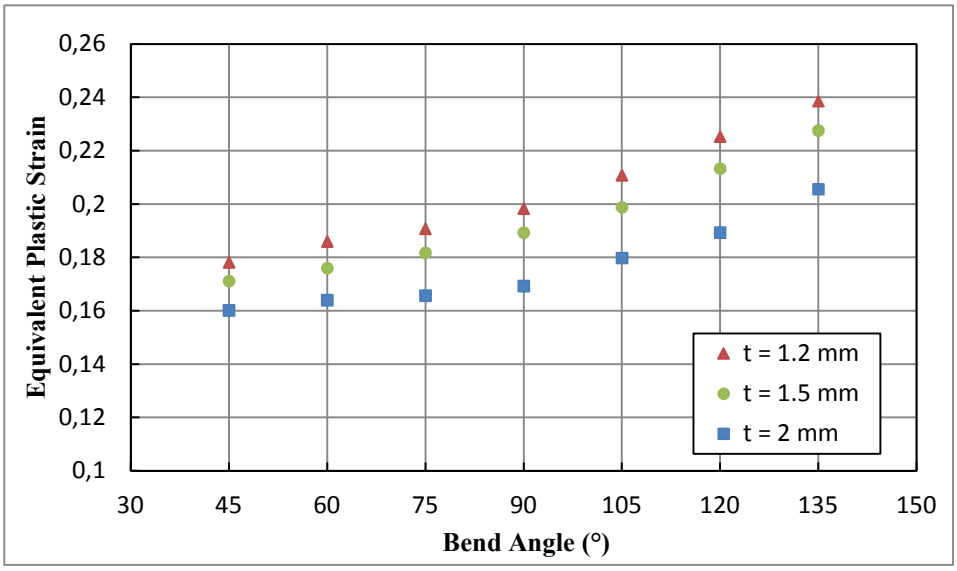

Figure 5-8 Maximum Equivalent Plastic Strain vs Bend Angle for St37 Tubes

5.2.2 Wall Thickness Changes of St37 Steel Tubes

It is proven that, in a rotary draw bending maximum thinning of the wall occurs at extrados and maximum thickening occurs at intrados. Both considerations are plotted as wall thickness change percentages in the following sections.

3 different tube bending experiments have been performed for each different wall thickness of the St37 tubes with 7 different rotary draw bending simulations. After performing the experiments, bent tubes were cut through their half bend angle sections and wall thicknesses were measured at the intrados and extrados. Afterwards wall thinning and wall thickenings were calculated in percentages.

5.2.2.1 Wall Thickness 1.2 mm

Wall thickness changes obtained by simulations and bending experiments of St37 Steel tubes for 1.2 mm wall thicknesses are presented in Figure 5-9.

Maximum thickening has been observed at 135° bend angle and it was 13.4% whereas minimum thickening was 10.1% at 45° bend angle. Also minimum thinning is 9.5% at 45° and maximum thinning is -12.3% at 135° for the 1.2 mm wall thickness St37 tubes.

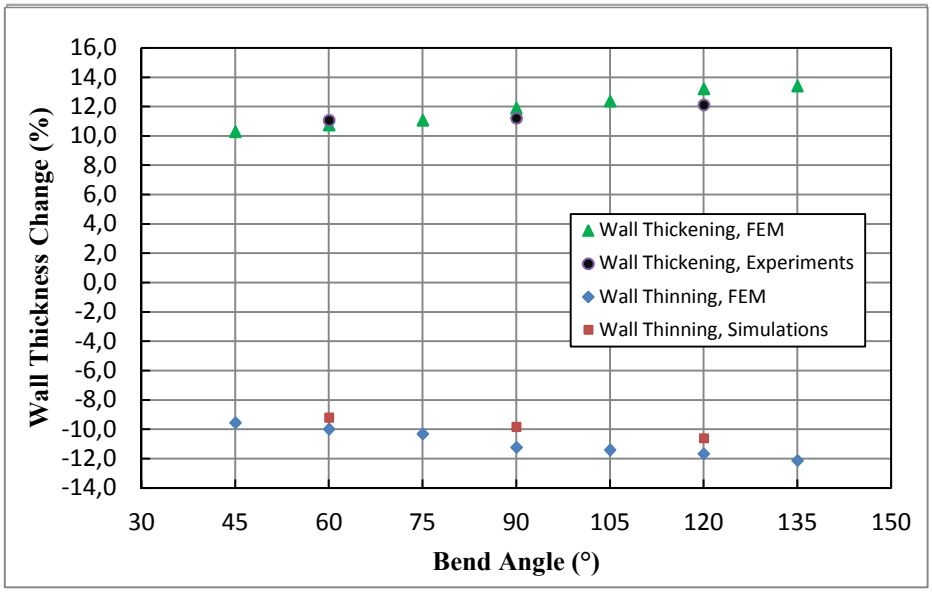

Figure 5-9 Wall Thickness Change vs Bend Angle for St37 Steel Tubes having 1.2 mm Wall Thicknesses

In experiments, maximum thickening and maximum thinning has been obtained by the 120° bending operation, and maximum thickening was 12.2% and maximum thinning was -10.6%. Also minimum thickening was 11% whereas minimum thinning was -9.2 at 60° bending experiment.

Maximum deviation for thickening between the simulation results and experiment results was encountered in 120° bending. The difference between the experiment result and simulation result is 9.1% at that bending angle. On the other hand, maximum thinning deviation observed at results of 90° bending. The difference between is 14.2% at 90° bending. For 1.2 mm wall thickness tubes, both wall thinning and wall thickening values increase with increasing bend angle.

5.2.2.2 Wall Thickness 1.5 mm

In Figure 5-10 experimental results and simulation results are compared for 1.5 mm wall thickness. Maximum wall thickening was 12.3% which has been seen at 135° and minimum thickening was 8.1% at 45° bend angle. Minimum thinning has been seen at 45° which is -7.6% and a maximum of -10.6% wall thinning has been observed at 135°. Moreover, in the experiments minimum thinning has been obtained by 60° bending which was -8.7% whereas maximum thinning was -9.5% at 120° bending. Also, minimum thickening was 9.7% which was seen at 60° and maximum thickening was 11.6 which were seen at 120°.

Moreover, in the analysis of 1.5 mm wall thickness St37 Steel tubes, maximum wall thinning deviation between the simulation and the experiment results is seen at 120° bending. At that bending angle there is 7.8% difference between the experimental and simulation result. On the other hand, maximum deviation between the wall thickening results was observed at 90° bending. 13.1% wall thickening deviation occurred between the related experimental and simulation results. It is seen that, wall thickening and wall thinning values tubes have an increasing tendency with increasing bend angle.

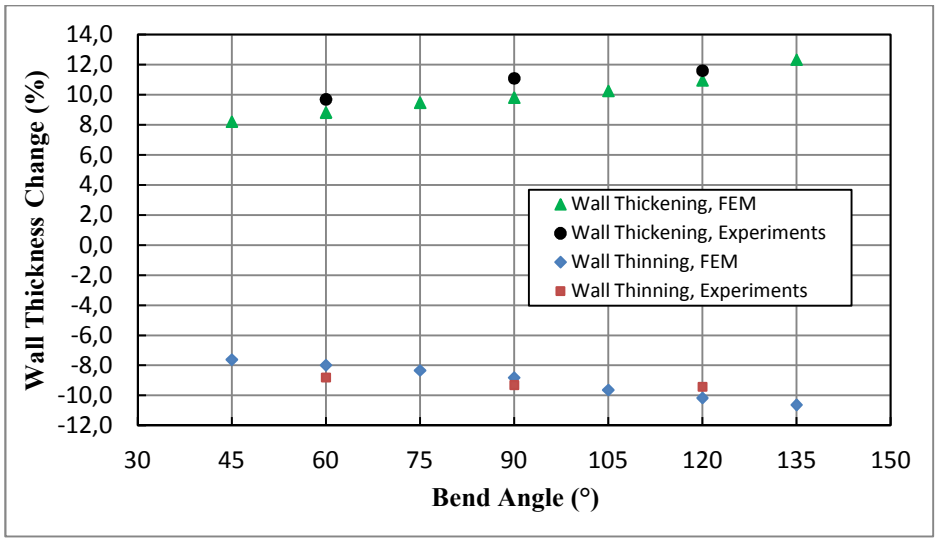

Figure 5-10 Wall Thickness Change vs Bend Angle for St37 Steel Tubes having 1.5 mm Wall Thicknesses

5.2.2.3 Wall Thickness 2 mm

The experiment and simulation results are presented in Figure 5-11.

Maximum wall thickening and maximum wall thinning has been observed at 135° in simulations. Maximum thinning and maximum thickening were -8.8% and 9.7%, respectively. Minimum thinning and also minimum thickening were seen at 45°. Minimum thinning was -7.1% and minimum thickening was -7.5%.

When the experiment and simulation results of 2.0 mm wall thickness St37 Steel tubes are considered, it is seen that maximum deviation between wall thinning results has come up at 120° bending. The difference between the percentage wall thinning values was 9.8% at the related bend angle. Maximum deviation in the wall thickening values was observed at 90° bending; the difference between the experimental result and simulation results is 12.9%.

5.2.2.4 Comparison of Wall Thickness Changes

Wall thickness variation values are compared with each other; wall thickening results are given in Figure 5-13 and wall thinning results are given in Figure 5-12 which shows that when wall thicknesses of the tubes increase wall thinning ratios decrease. Both experimental and simulation data are plotted, they have similar tendencies with increasing wall thickness. Figure 5-13 illustrates that the wall thickening percentages decrease with increasing tube wall thicknesses. Both experimental and simulation results have decreasing profiles.

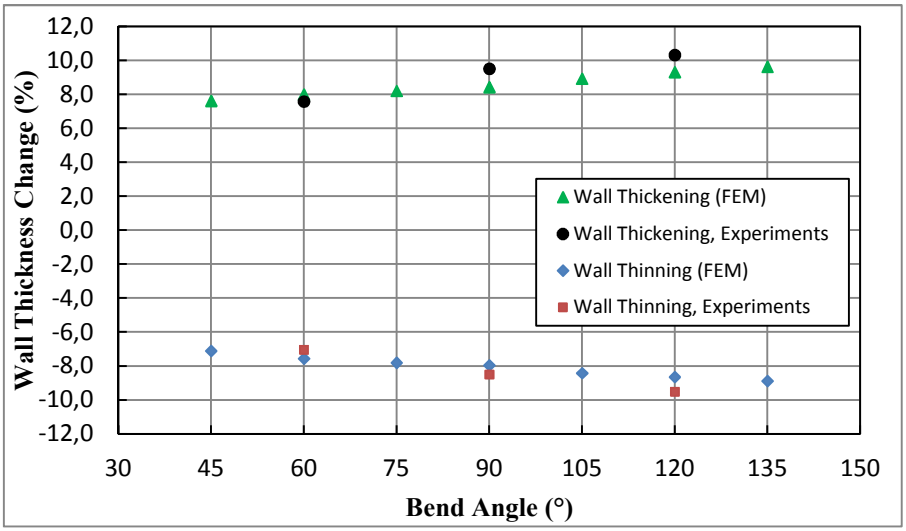

Figure 5-11 Wall Thickness Change vs Bend Angle for St37 Steel Tubes having 2.0 mm Wall Thicknesses

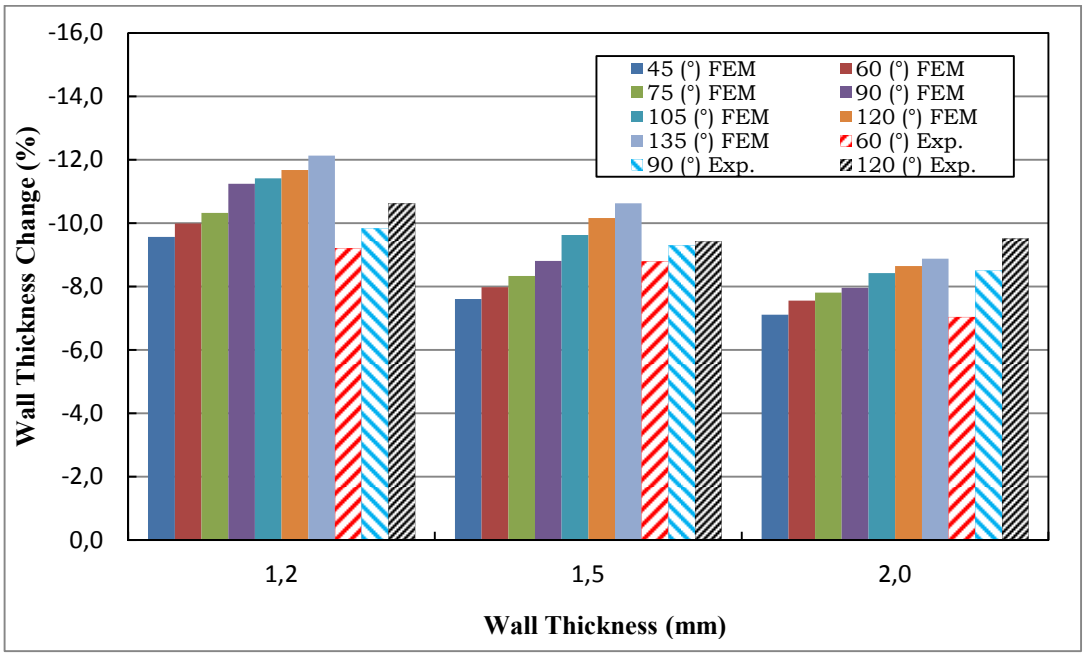

Figure 5-12 Wall Thickness vs Wall Thinning for St37 Tubes

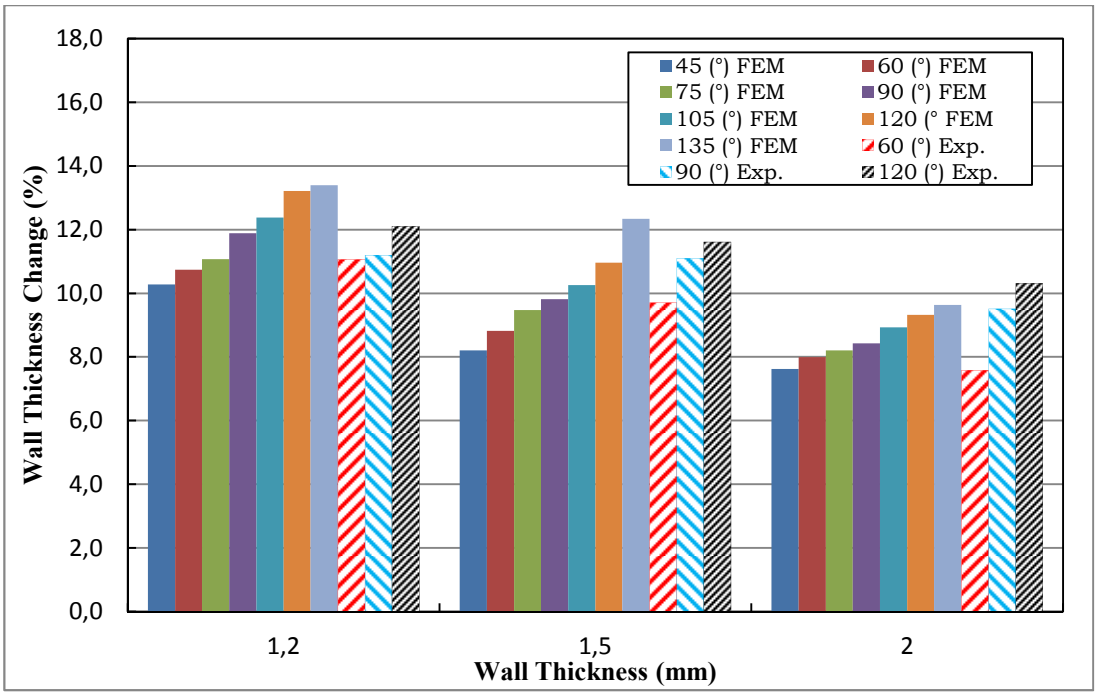

Figure 5-13 Wall Thickness vs Wall Thickening for St37 Tubes

5.2.3 Cross Section Distortions of St37 Steel Tubes

To make a precise comparison for the cross-section distortions of the bent tubes, ovalization parameters are investigated. Ovality values are directly related to the quality of the bending. The less ovalization, the more quality bending achieved. Rotary draw bending process is a flexible and easy to apply process but it does not have the best cross-section distortion values concerning the other bending techniques. Therefore, if less ovalization values are desired, some other techniques could be used such as hydroforming or rotary draw bending with push assistant loadings. In this section, ovality values for the rotary draw bending process obtained by the finite element solutions and experiments are compared.

In order to get the maximum and minimum distorted diameters, the ovality values are determined at their half bend angle planes at the end of the finite element simulation as illustrated in Figure 5-14. At higher bend angles the distortion of the bent tubes can be visualized more easily. A schematic view of the distorted cross-section is shown on Figure 5-15 for 120° bend angle.

After investigating half bend angle sections of the tubes maximum and minimum distorted diameters are measured and ovality percentages are calculated for each tube. Cross-section distortion results are handled in three parts and 7 simulation data and 3 experiment measurements exist for 3 different wall thicknesses of the St37 Steel tubes.

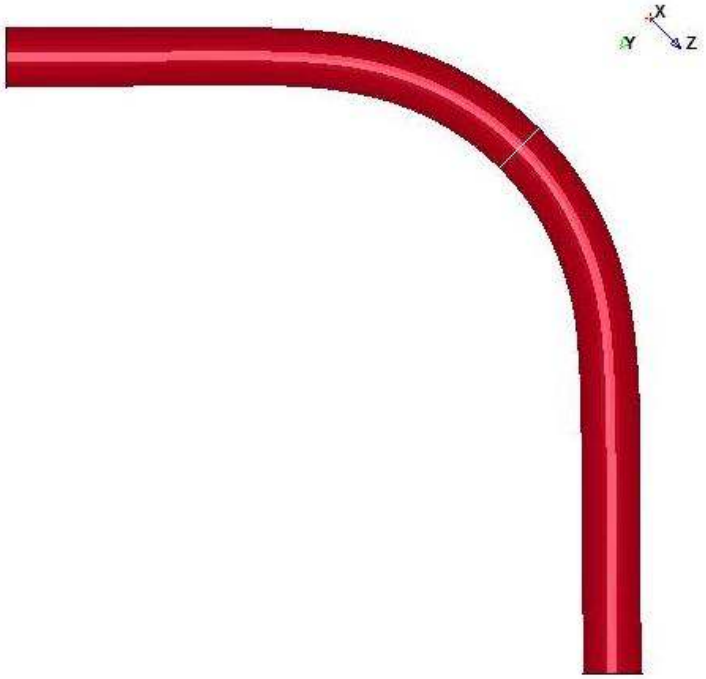

Figure 5-14 Cutting of the 90˚ Bent Tube from its Half Bend Angle

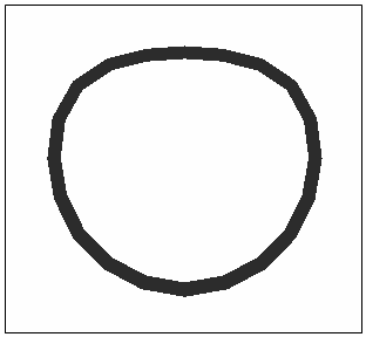

Figure 5-15 Shape of the Cross-section after Bending Operation

5.2.3.1 Wall Thickness 1.2 mm

The ovality results with respect to bend angle for the 1.2 wall thickness tubes are illustrated in the Figure 5-16.

Maximum ovality was obtained as 12.0% at 135° bend angle. The minimum ovality value was obtained at 45° and it was 8.9% in the simulations. However, in the experiments maximum value was obtained at 120° which is 13.1% and minimum experimental value was 10.1% at 60° bending.

The analysis of 1.2 mm wall thickness St37 Steel tubes showed that the maximum deviation between the experiment and simulation values was observed at 120° bending. The deviation between the experimental and simulation results came up as 14.1%. Results also illustrate that, as the bend angle increases ovality values increase too.

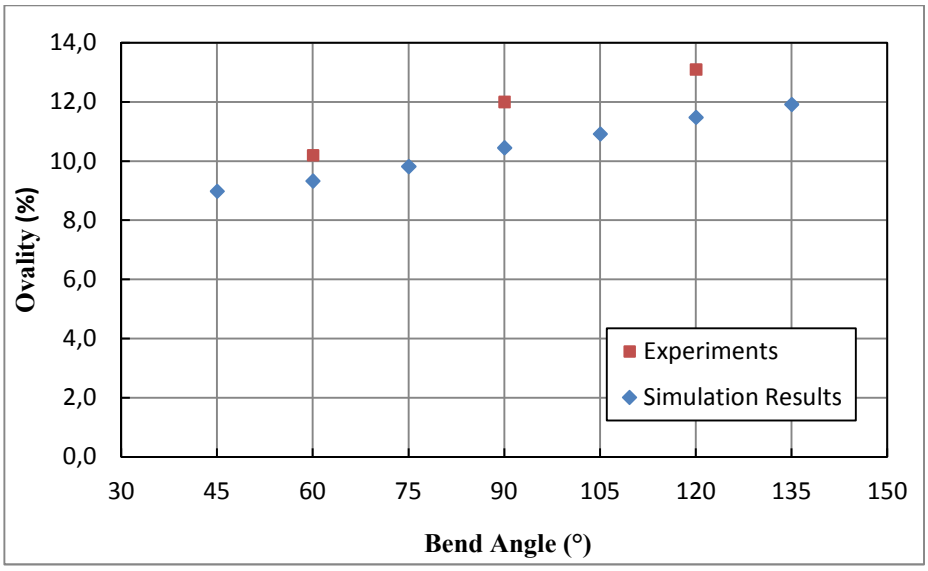

Figure 5-16 Ovality vs Bend Angle for St37 Steel Tubes having 1.2 mm Wall Thicknesses

5.2.3.2 Wall Thickness 1.5 mm

Figure 5-17 shows the variation of the ovalization values of the St37 Steel tubes having 1.5 mm wall thicknesses with respect to the bend angle. Numerical simulation shows that, the maximum ovality was 11.4% for 135° bend angle whereas the minimum ovality was obtained for 45° bend angle as 8.4%. For the experiments, minimum ovality was 10.1% at 60° bend angle whereas maximum ovality was 11.7% for 120° bend angle.

The maximum deviation was 14.6%, has been observed at 60° bending angle between the results of simulations and experiments. It is seen that, as the bend angle gets higher, the cross-section distortion of the tubes gets larger.

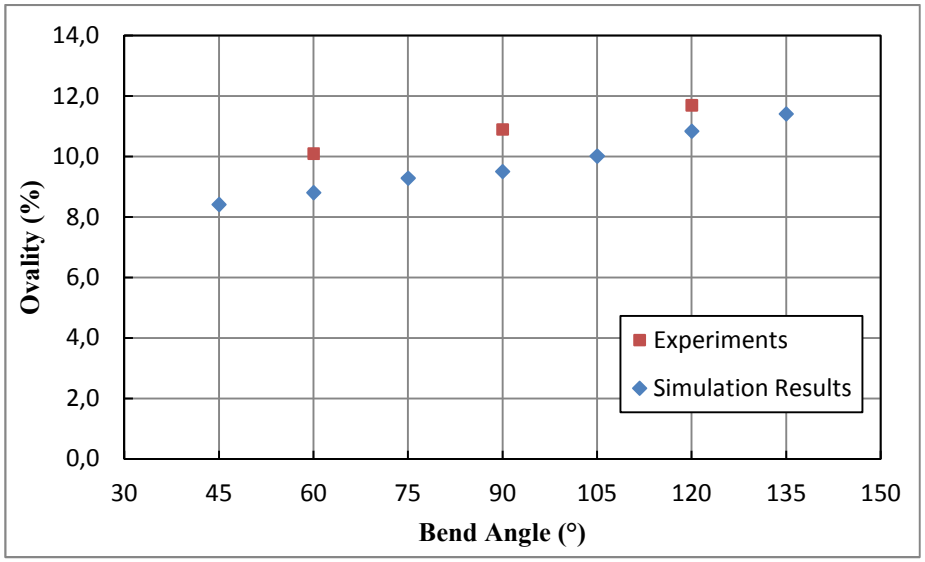

Figure 5-17 Ovality vs Bend Angle for St37 Steel Tubes having 1.5 mm Wall Thicknesses

5.2.3.3 Wall Thickness 2 mm

Figure 5-18 is prepared for the comparison of the ovality values taken from the finite element solution and experimental measurements for the 2 mm wall thickness St37 Steel tubes.

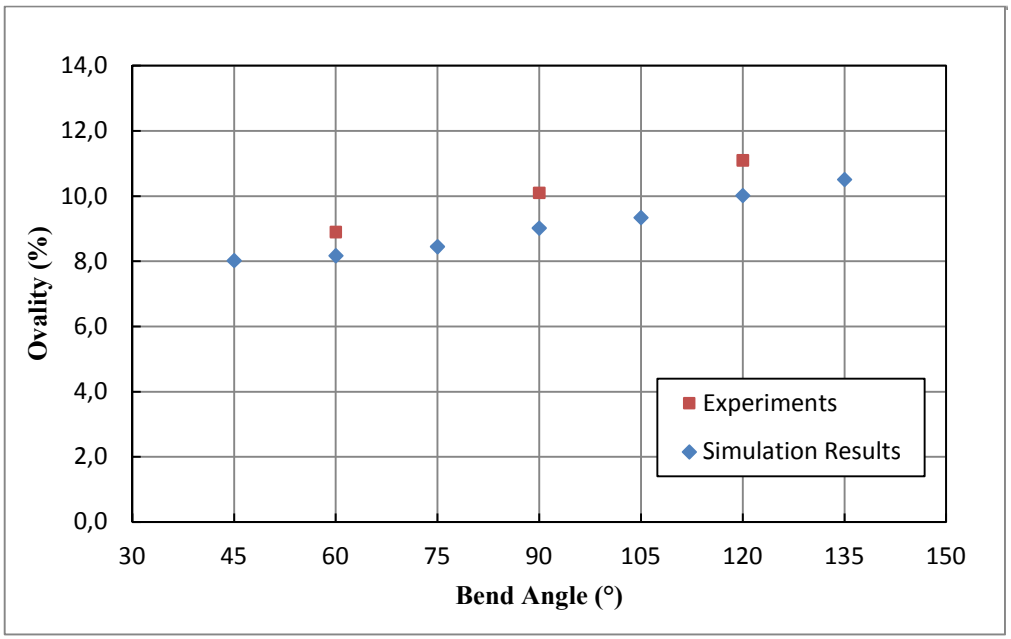

Figure 5-18 Ovality vs Bend Angle for St37 Steel Tubes having 2.0 mm Wall Thicknesses

According to numerical results, maximum ovality has been obtained by 135° bending and it was 10.5%. Also minimum ovality value has been observed at 45° bending as 8.0%. In the experiments, maximum ovality was 11.1% for 120° bend angle and minimum ovality was 8.8% for 60° bending.

The analysis performed for the 2 mm wall thickness St37 Steel tubes illustrated that maximum deviation was occurred at 120° bending. Deviation between the experiment and simulation results is 11.8 % at that bend angle. The ovality values increases with increasing bend angle for the 2 mm wall thickness St37 tubes.

5.2.3.4 Comparison of Ovalities

All three thickness values were considered together and the results were shown in Figure 5-19.

According to Figure 5-19, ovality results obtained by the experiments and the simulations have a decreasing profile with the increasing wall thickness. In other words, to have less cross-section distortion, thicker tubes should be used.

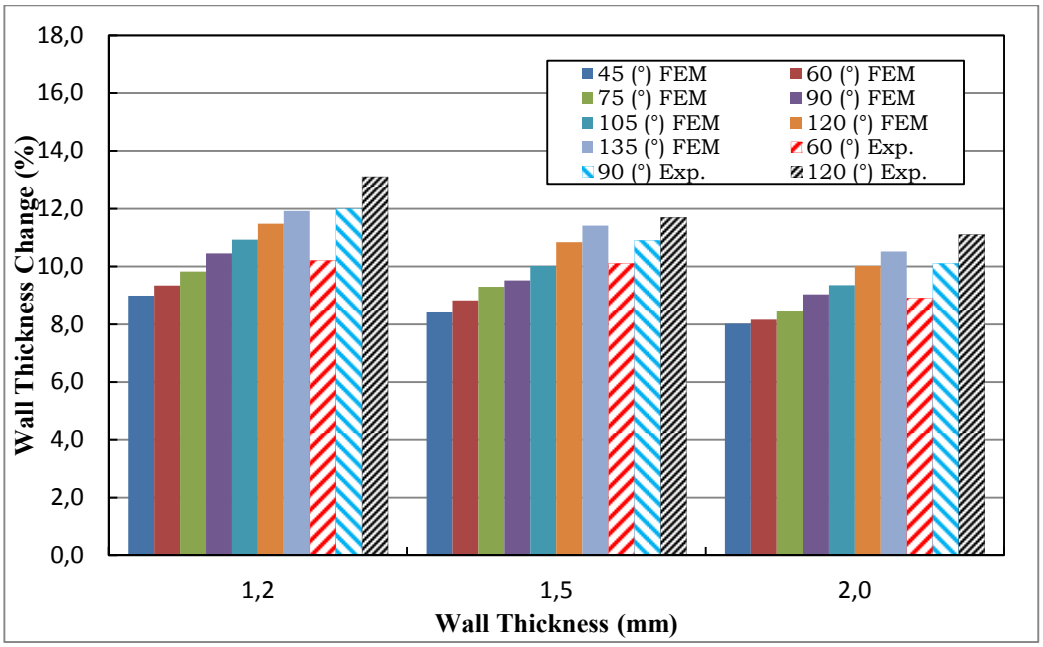

Figure 5-19 Wall Thickness vs Ovalities for St37 Tubes

5.2.4 Spring-back Angles of St37 Steel Tubes

To simulate spring-back implicit analysis is performed. The results of the explicit analysis, such as tube thicknesses, nodal displacements stress and strain values, has been obtained at the end of the bending operation and used as input for the implicit analysis.

Shell model is used for the implicit analysis too. However, since different element types are available for explicit analysis and implicit analysis, a different shell element is used. Spring-back simulations have been performed for all explicit bending simulations. Sample spring-back solution of the St37 Steel tube with 1.5 mm wall thickness is illustrated in Figure 5-20.

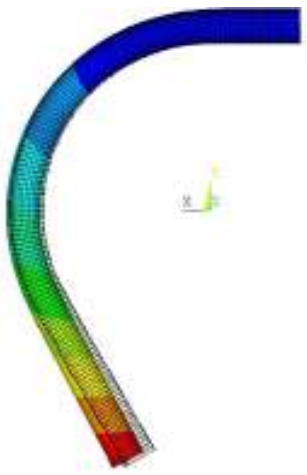

Figure 5-20 Sample Spring-back Solution of the St37 Tube

In Figure 5-20 both configurations of the bent tube; before and after spring-back are illustrated. Spring-back angle results were handled for three different wall thickness values.

5.2.4.1 Wall Thickness 1.2 mm

Spring back angles of the St37 Steel tubes of 1.2 mm wall thicknesses are plotted in Figure 5-21 with respect to different bend angles which are starting from 45° and increasing with the increment of 15°.

According to simulation results, maximum spring-back angle has been seen at 135° bending and it was 1.5°. Also, minimum spring-back was observed at 45° bending as 0.5°. Furthermore, in the experiments, maximum spring-back amount was 1.4° for 120° bend angle whereas minimum spring-back angle was 0.5° at 60° bend angle.

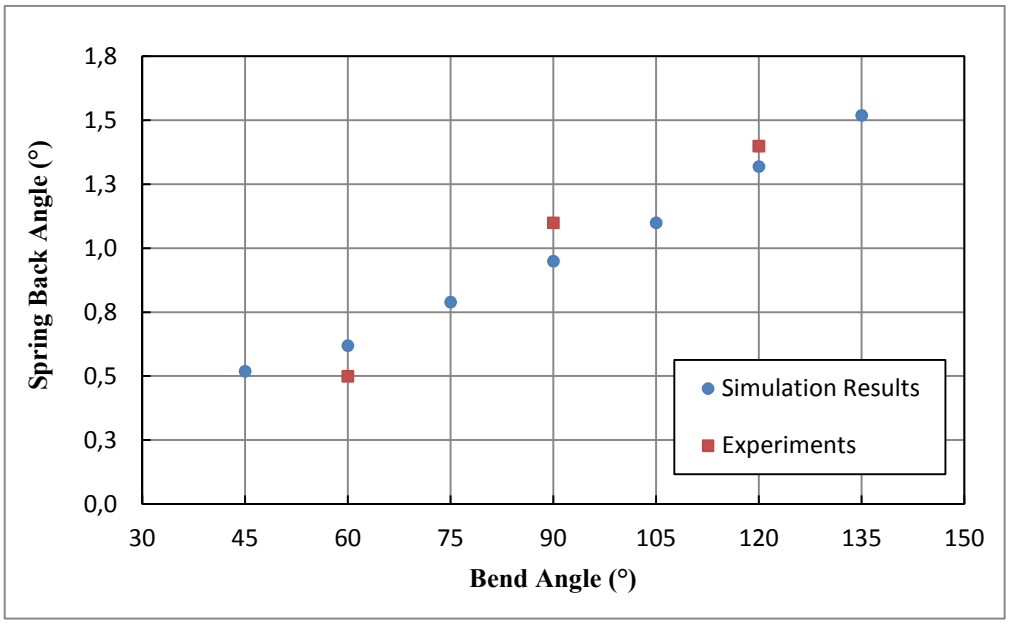

Figure 5-21 Spring-back Angle vs Bend Angle for St37 Steel Tubes having 1.2 mm Wall Thicknesses

5.2.4.2 Wall Thickness 1.5 mm

Figure 5-22 shows the spring-back results of 1.5 mm wall thickness St37 Steel tubes. Experiment results and simulation data are compared in the plot. Maximum spring-back angle was 2.3° for 135° bend angle, minimum spring-back angle was 0.95° for 45° bend angle in the numerical results. Also, in the experiments maximum spring-back angle has been seen at 120° bending and it was 2.0° and minimum spring-back angle has been observed at 60° bending and it was 1.1°.

Maximum deviation between the experiment and simulation results, which was about 13.1%, has been observed at 90° bending. The simulation results of 1.5 mm wall thickness St37 tubes show that, the spring-back angles increase almost linearly with increasing bend angle.

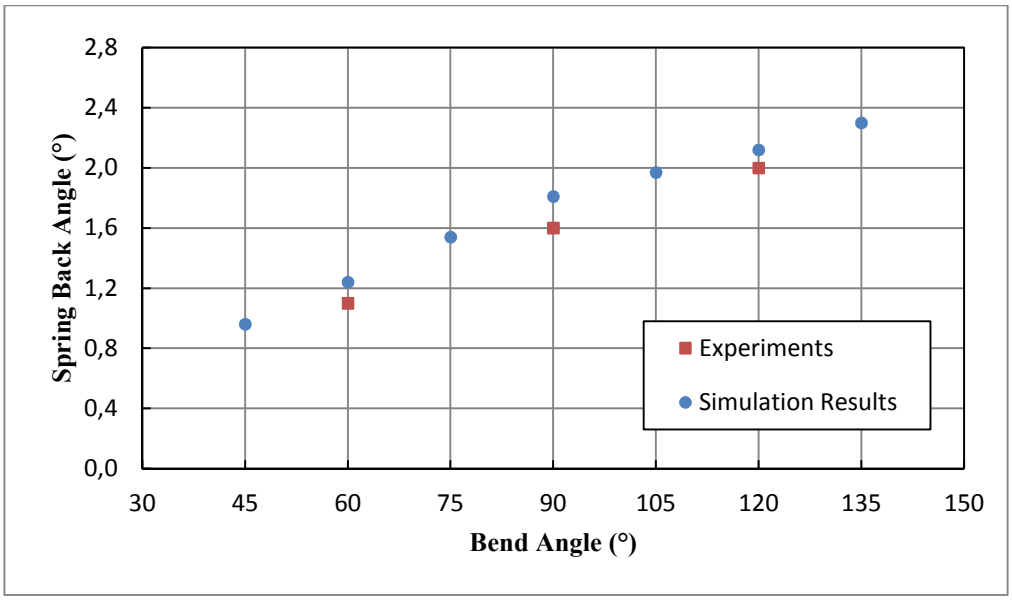

Figure 5-22 Spring-back Angle vs Bend Angle for St37 Steel Tubes having 1.5 mm Wall Thicknesses

5.2.4.3 Wall Thickness 2 mm

The results for St37 Steel tubes with 2.0 mm wall thicknesses are presented in the Figure 5-11. When the simulation results are considered, it is seen that the maximum spring-back angle was 2.85° which is for 135° bend angle and minimum spring-back angle was obtained by 45° bending simulation which is 1.4°.

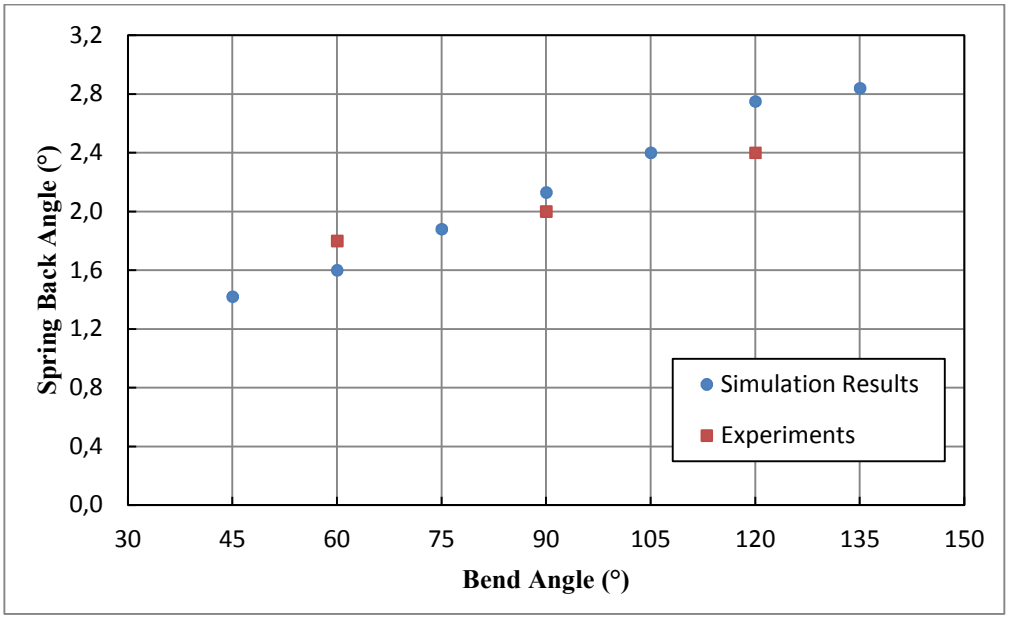

Figure 5-23 Spring-back Angle vs Bend Angle for St37 Steel Tubes having 2.0 mm Wall Thicknesses

Figure 5-23 shows, the maximum deviation between the experimental and finite element results has been observed at 120° bending. The difference was 12.8% between experimental measurement and simulation result at that bend angle. The other results also imply that, spring-back angles have an increasing tendency, with increasing bend angle, which is almost linear.

5.2.4.4 Comparison of Spring-back Angles

In Figure 5-24 spring-back angle variations with respect to the wall thicknesses are shown. It is seen that spring-back amounts increase with increasing wall thickness of the tubes.

When all the results for St37 tubes are put together, it is realized that wall thickness changes and cross-section distortion values decrease with increasing wall thickness but, spring-back angles increase with increasing wall thickness.

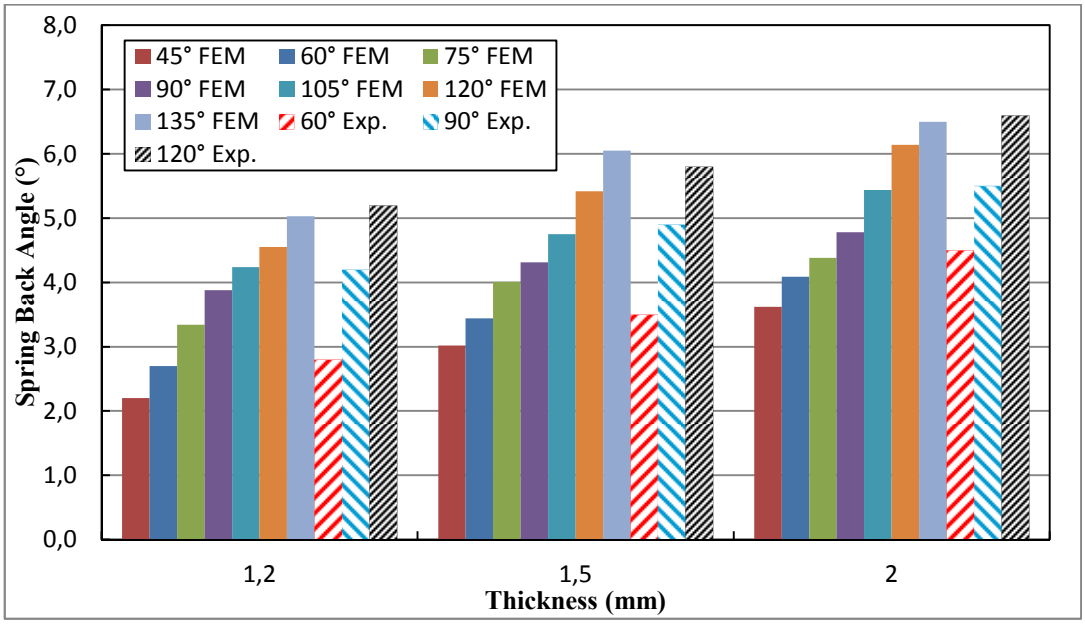

Figure 5-24 Wall Thickness vs Spring-back for St37 Tubes

5.3 Results for SS304 Stainless Steel Tubes

Same procedure with the St37 Steel tubes (i.e. obtaining the finite element and experiment results) is followed for the SS304 Stainless Steel tubes. The number of experiments, explicit and implicit analysis is kept same. Stress and strain results, wall thickness changes, cross-section distortions and spring-back angle results are explained in the next sections.

5.3.1 Stress and Strain Variations of the SS304 Stainless Steel Tubes

Maximum equivalent stress and strain occurs at extrados. Von-Mises stress at extrados is plotted in Figure 5-25 for SS304 Stainless Steel tubes. Results for different wall thicknesses are included in the figure. 21 simulations are performed for the SS304 tubes. 7 different bending simulation results have been obtained for each different wall thickness of the SS304 tubes same as St37 ones. Maximum von-Mises stress value for the 2 mm wall thickness tubes was obtained as 454.9 MPa in the bending simulations. They were 479.3 MPa for 1.5 mm wall thickness tubes and 495.7 for 2 mm wall

thickness tubes. The stress values get higher at higher bend angles and also they increase with decreasing wall thickness of the tubes. Maximum equivalent plastic strain values for the bending of SS304 Stainless Steel tube are illustrated in Figure 5-26, 3 different curves exist for 3 different wall thicknesses of the tubes.

Maximum equivalent plastic strain for the 1.2 mm wall thickness SS304 Stainless Steel tubes have come out as 0.184. It is 0.178 for the 1.5 wall thickness tubes and 0.170 for the 2 mm wall thickness tubes. Similar with the stress values, maximum strains in the bending region increases as the tube thicknesses decrease and also they increase with increasing bend angle.

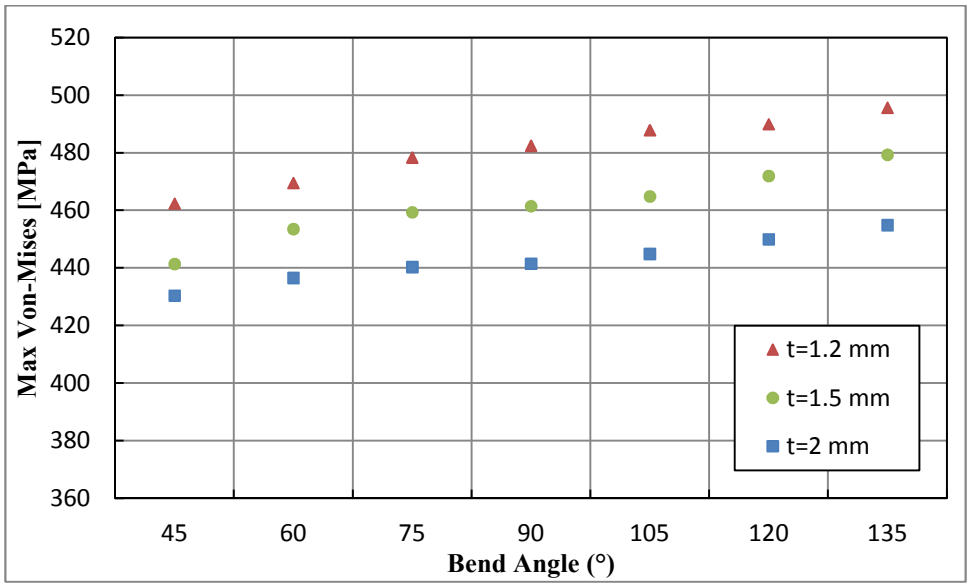

Figure 5-25 Maximum Stress vs Bend Angle for SS304 Tubes

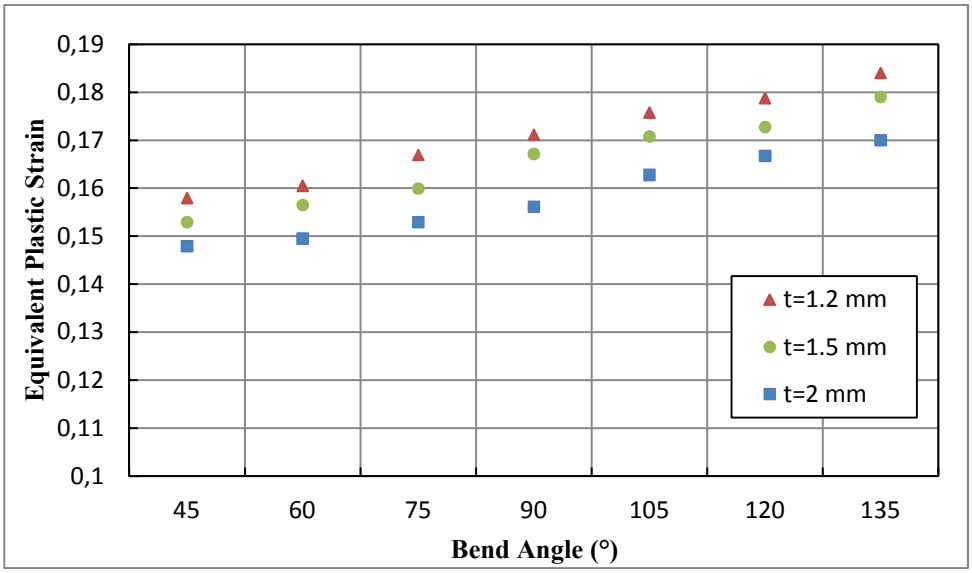

Figure 5-26 Maximum Equivalent Plastic Strain vs Bend Angle for St37 Tubes

5.3.2 Wall Thickness Changes of the SS304 Stainless Steel Tubes

Results are presented in the following sections according to tube wall thickness values. After that the effect of the tube wall thicknesses to wall thickness change is discussed.

5.3.2.1 Wall Thickness 1.2 mm

Wall thinning at extrados and wall thickening at intrados of the 1.2 mm wall thickness SS304 Stainless Steel tubes are plotted in Figure 5-27.

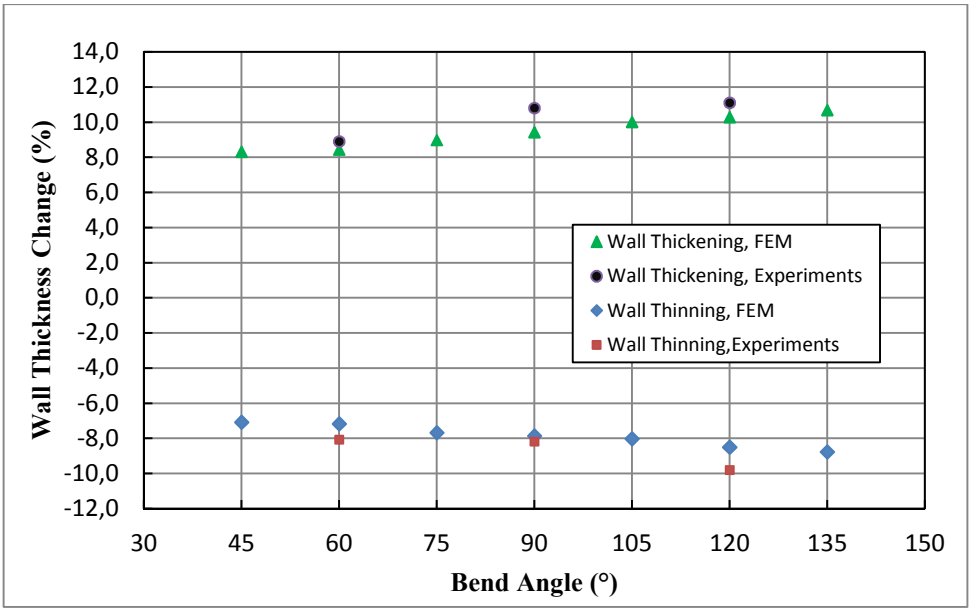

Figure 5-27 Wall Thickness Change vs Bend Angle for SS304 Tubes having 1.2 mm Wall Thicknesses

In the numerical solutions, maximum wall thickening was 10.7% for 135° bend angle and minimum thickening was 8.3% for 45° bend angle. Maximum thinning was -8.8% which has been obtained by 135° bending and minimum thinning was -7.1% which has been obtained by 45° bending simulation. Also, in the experiments minimum thickening was occurred at 60° bend angle as 8.8% and maximum thickening was 11.1% for 120° bend angle. Moreover, maximum thinning has been seen at 120° bending angle which was -9.8% and minimum thinning has been observed at 60° bending experiments as -8.0%.

When the results are considered it is seen that maximum deviation between the wall thickening results, 13.9%, has occurred at the 90° bending. Also, maximum deviation at wall thinning results has come up at 120° bending which was 14.2%. Wall thickness changes of the 1.2 mm wall thickness SS304 tubes increases with the increasing bend angle.

5.3.2.2 Wall Thickness 1.5 mm

The results for the 1.5 mm tubes obtained and maximum wall thinning and maximum wall thickening values are illustrated in the same plot in Figure 5-28.

Considering the simulation values, it is seen that, maximum thickening was 9.6% for 135° bend angle whereas minimum thickening was 7.1% for 45° bend angle. On the other hand, maximum thinning was -8.0% for 135° bend angle and minimum thinning was -6.6% for 45° bend angle. In the experiments, maximum thickening was 10.3% for 120° bend angle and minimum thickening was 8.7% for 60° bending experiment. Furthermore, minimum thinning was -7.7% for 60° bending experiment and maximum thinning was -8.7% for 120° bending experiment.

When the experiment and simulation results are considered, it is seen that maximum deviation between wall thinning results has occurred at 90° bending. The deviation between the related results is 13.8%. In addition, maximum deviation in the wall thickening values has been observed at 120° bending; which is resulting in a deviation of 8.9% between the experiment and simulation results. It is also realized that wall thinning and wall thickening values increase with increasing bend angle.

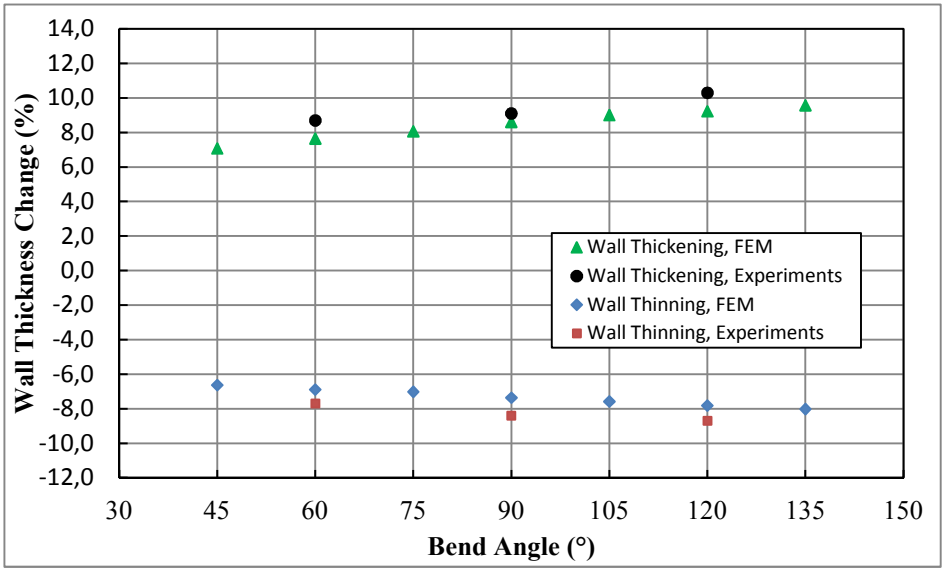

Figure 5-28 Wall Thickness Change vs Bend Angle for SS304 Tubes having 1.5 mm Wall Thicknesses

5.3.2.3 Wall Thickness 2.0 mm

Similarly, all results for 2.0 mm exist in Figure 5-29. From the simulation results, it has been observed that, maximum wall thickening value was 8.4% for 135° bend angle and minimum thickening was 6.1% for 45° bending. Also, minimum thinning was -6.1% for 45° bend angle and maximum thinning was -7.3% for 135° bend angle. However, in the experiments maximum thickening was 8.6% for 120° bend and minimum thickening was 7.1% for 60° bend angle whereas maximum thinning was -7.9% for 120° bending experiment and minimum thinning was -6.1% for 60° bending experiment.

5.3.2.4 Comparison of Wall Thickness Changes

After that, wall thickening and wall thinning values are considered with respect to the tube wall thicknesses in Figure 5-30 and Figure 5-31 by using the results belonging to all bend angles. The experimental and simulation results show that wall thickening and wall thinning percentages decrease with increasing tube wall thicknesses. It is also seen that, wall thinning and wall thickening values increase with increasing bend angle both for the experimental and simulation results.

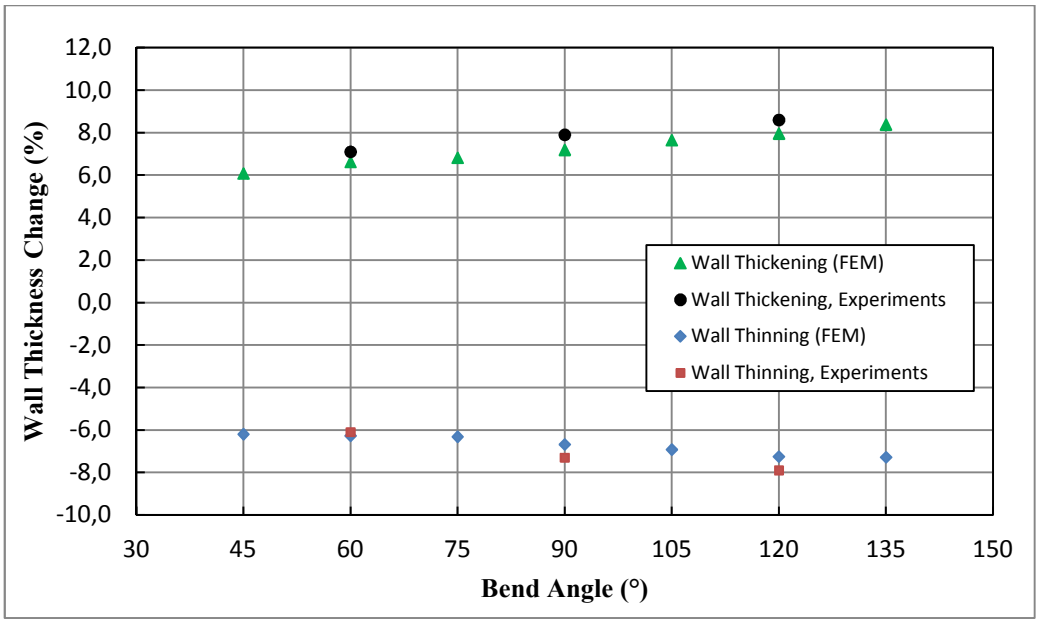

Figure 5-29 Wall Thickness Change vs Bend Angle for SS304 Tubes having 2.0 mm Wall Thicknesses

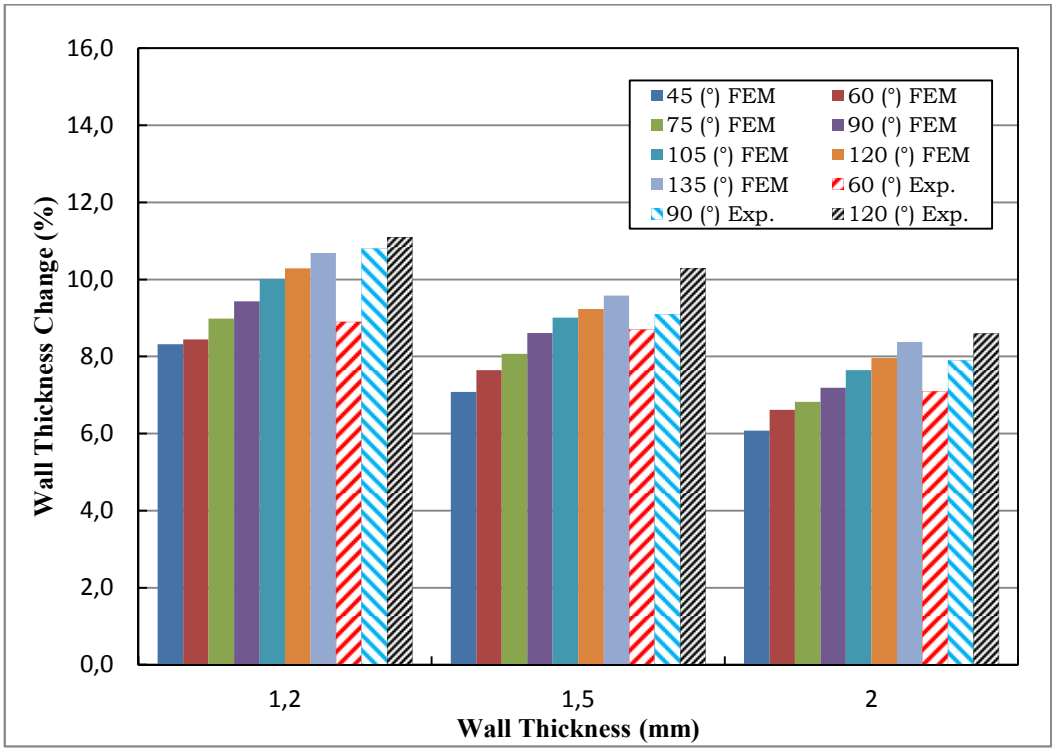

Figure 5-30 Wall Thickness vs Wall Thickening for SS304 Tubes

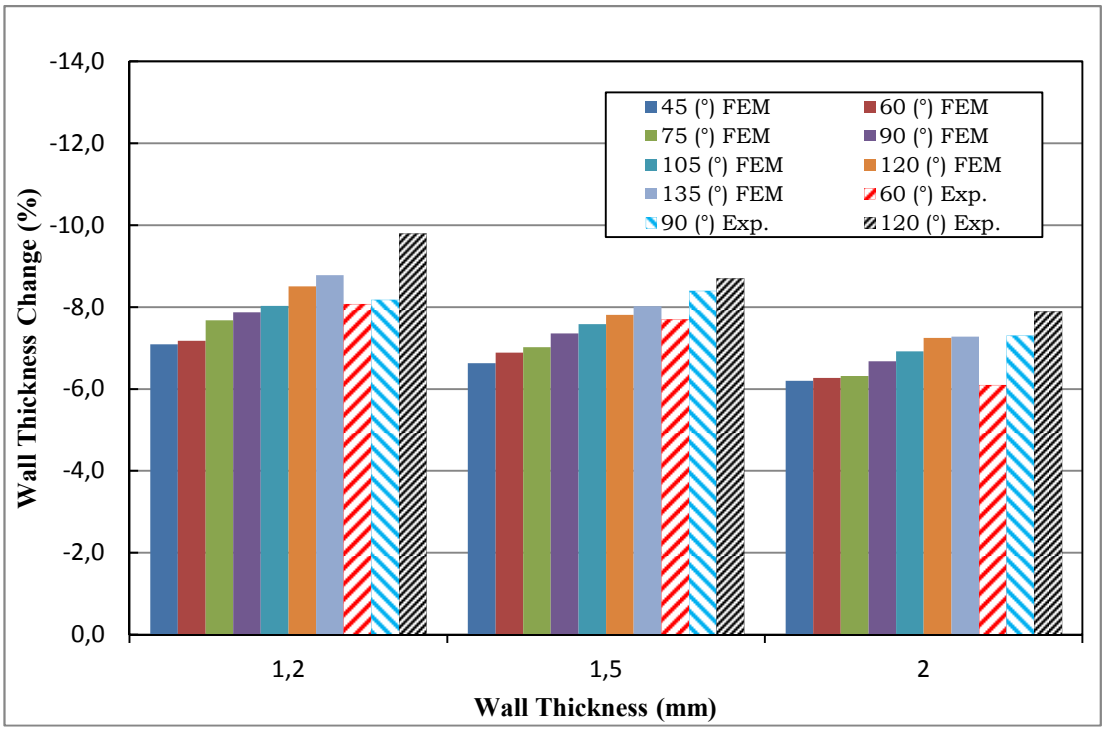

Figure 5-31 Wall Thickness vs Wall Thinning for SS304 Tubes

5.3.3 Cross-section Distortion for SS304 Steel Tubes

After the rotary draw bending experiments has been finished the SS304 Stainless Steel tubes were cut through their half bend angle section to observe the maximum cross-section distortion in the bent tubes.

5.3.3.1 Wall Thickness 1.2 mm

Figure 5-32 shows the change of the ovality values of the SS304 Stainless Steel tubes with 1.2 mm wall thicknesses with respect to the bend angle.

Simulation results show that, maximum ovality value was occurred as 9.4% for 135° bend angle whereas minimum ovality value was 6.9% for 45° bending solution. However, in the experiments maximum ovality value was 10.3% for 120° bending experiment and minimum ovality value was 8.3% for 60° bending experiment.

Maximum deviation between the simulation and experimental data come up at 120° bending. At 120° bending the difference between the simulation and experimental data is 10.8%. The experimental and simulation results both increase with the increasing bend angle for the 1.2 mm SS304 tubes.

5.3.3.2 Wall Thickness 1.5 mm

Similar plot is prepared for the SS304 Stainless Steel tubes having 1.5 mm wall thicknesses. Results are illustrated in Figure 5-33.

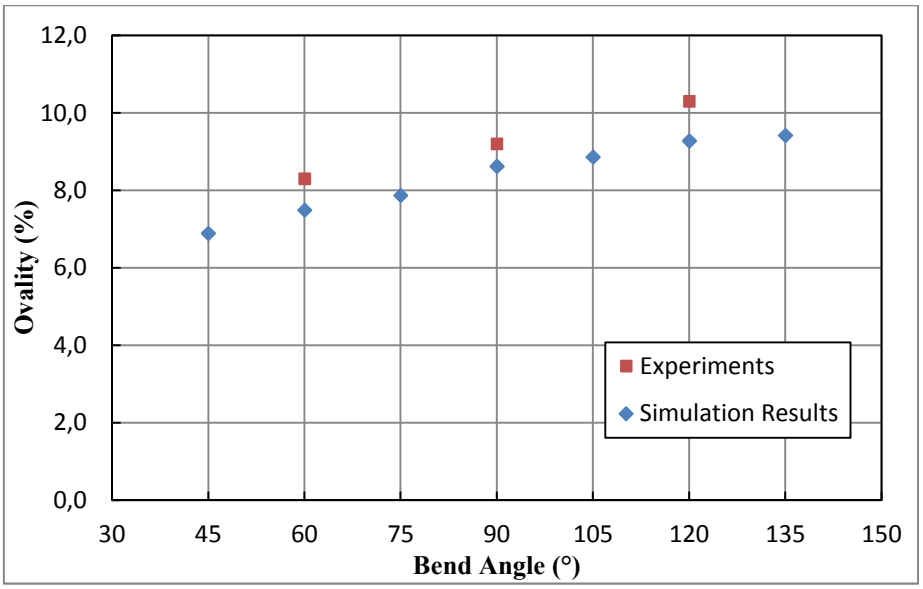

Figure 5-32 Ovality vs Bend Angle for SS304 Steel Tubes having 1.2 mm Wall Thicknesses

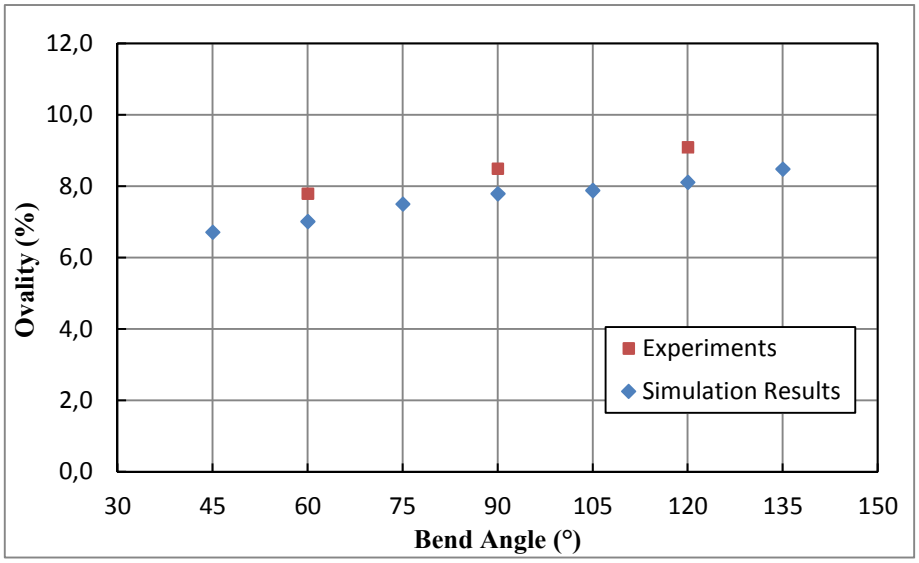

Figure 5-33 Ovality vs Bend Angle for SS304 Steel Tubes having 1.5 mm Wall Thicknesses

Maximum ovality value has been obtained as 8.5% for 135° bending simulation and minimum ovality value was 6.7% for 45° bending simulation whereas in the experiments, maximum ovality value was 9.1% for 120° bending experiment and minimum ovality was 7.8% for 60° bending experiment.

Maximum deviation between the ovality values, which is 12.8%, has seen at 120° bending. When the results are taken into account, it is observed that the cross-section distortion of the 1.5 mm tubes increases as the bend angle increases.

5.3.3.3 Wall Thickness 2 mm

Lastly, cross-section results of 2.0 mm wall thickness SS304 Stainless Steel tubes are shown in Figure 5-34. From the numerical results, maximum ovality value was 8.2% for 135° bend angle and minimum ovality value was 6.2% for 45° bend angle. Also, in experiment results, minimum ovality value was 6.9% for 60° bend angle whereas maximum ovality value was 8.2% for 120° bend angle.

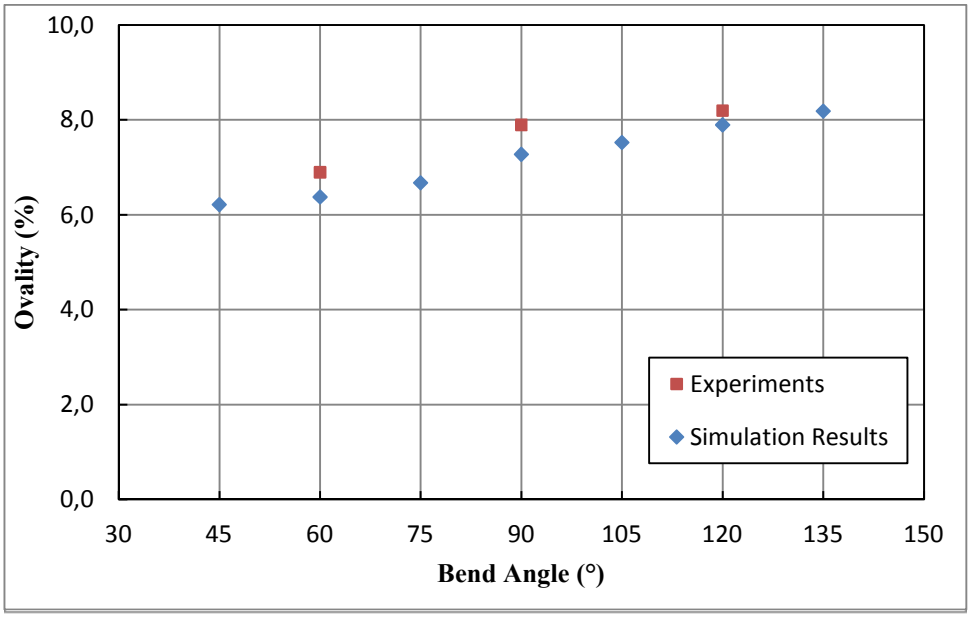

Figure 5-34 Ovality vs Bend Angle for SS304 Steel Tubes having 2.0 mm Wall Thicknesses

According to the ovality results presented in Figure 5-34, maximum deviation occurs at 90° bending. The deviation between the experimental measurements and simulation result is 8.4%, which shows that the results are in good agreement.

5.3.3.4 Comparison of the Cross-section Distortions

The effect of the wall thickness to cross-section distortions can be observed at Figure 5-35. It is seen that the ovality values of the SS304 tubes decreases with increasing tube wall thicknesses. Also, as the bend angle increases, the cross-section distortions of the bent tubes increase as well.

5.3.4 Spring-back Simulations for SS 304 Stainless Steel Tubes

The spring-back solution of a SS304 Stainless Steel having 1.5 mm wall thickness 120˚ bent tube is presented in Figure 5-36 as a sample simulation. Before and after spring-back states of the bent tube can be seen in figure. Spring-back results are put together in the following sections for the 1.2 mm, 1.5 mm and 2 mm wall thickness tubes, respectively.

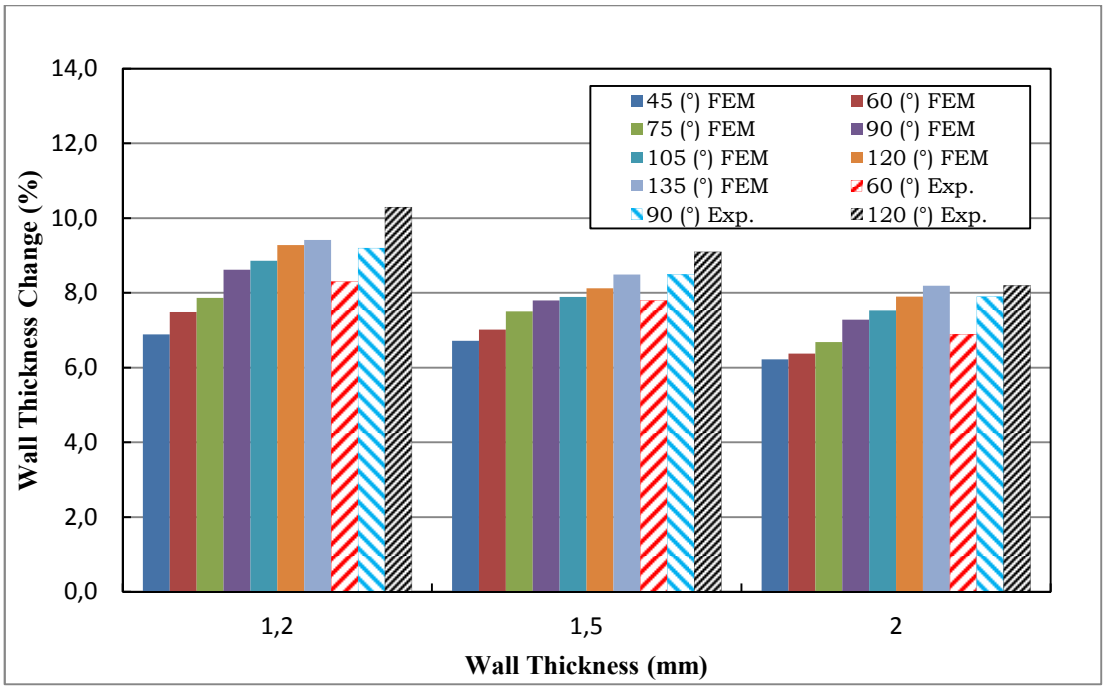

Figure 5-35 Wall Thickness vs Ovalities for SS304 Tubes

5.3.4.1 Wall Thickness 1.2 mm

Experimental and simulation results for the 1.2 mm SS304 tubes are illustrated in the Figure 5-37. From the simulations, maximum spring-back angle was found as 5.0˚ for 135˚ bend angle and minimum spring-back value was found as 2.2% for 45˚ bend angle. On the other hand, in the experiments maximum spring-back angle was observed as 5.2% in 120˚ bending experiment and minimum spring-back angle was observed as 2.8˚ in 60˚ bending experiment.

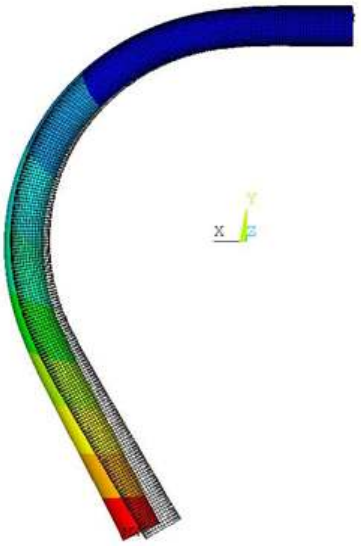

Figure 5-36 Spring-back Solution of the SS304 Stainless Steel 1.2 mm Wall Thickness Tube

14.2% difference, between the simulation and experiment results at 120° bending, was seen as the maximum deviation in the spring-back angles of the 1.2 mm wall thickness SS304 tubes. The spring-back angle results have an increasing profile which is almost linear.

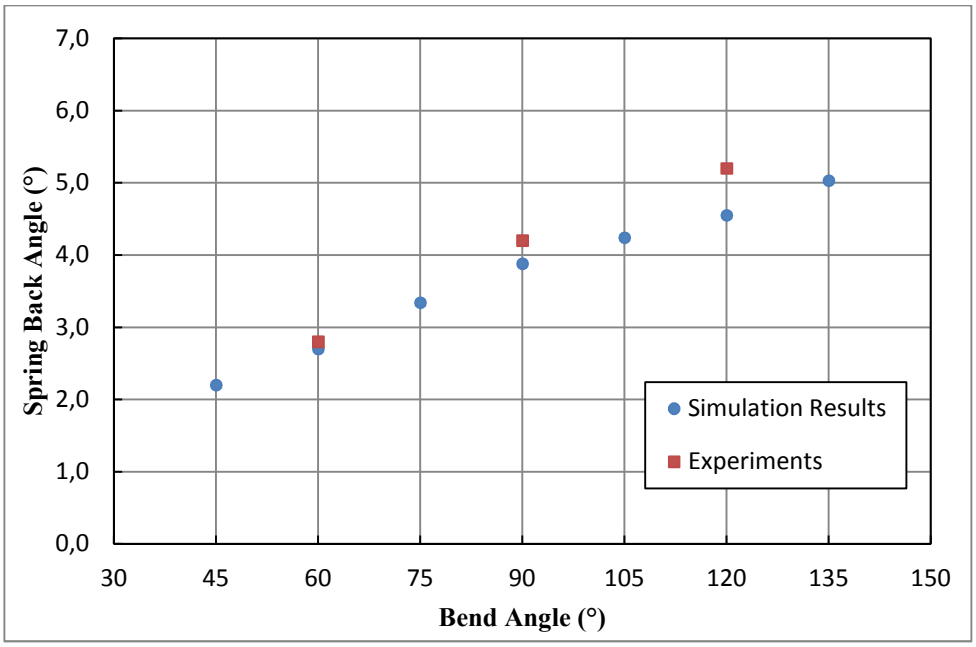

Figure 5-37 Spring-back Angle vs Bend Angle for SS304 Tubes having 1.2 mm Wall Thicknesses

5.3.4.2 Wall Thickness 1.5 mm

Results are plotted in Figure 5-38. In the simulations, maximum spring-back angle was 6.1° for 135° bend angle and minimum spring-back was 3.0° for 45° bend angle whereas maximum spring-back angle which was observed in 120° bending experiment is 5.8° and minimum spring-back angle which was observed in 60° bending experiment is 3.5°.

According to results, maximum difference between the simulation and experiment results was observed at 90° bending. The difference is about 13.6% which implies the simulation results are quite reasonable.

The results of 1.5 mm wall thickness SS304 tubes have an increasing tendency with increasing bend angle, which is almost linear.

5.3.4.3 Wall Thickness 2 mm

Spring-back results of 2.0 mm wall thickness SS304 Stainless Steel tubes are plotted in Figure 5-39. Maximum spring-back angle was 6.5° for 135° bend angle and minimum spring-back angle was 3.6° for 45° bending angle in the simulation results. Moreover, maximum spring-back angle was 6.6° for 120° bend angle and minimum spring-back angle was 4.5° for 60° bend angle in the experimental results. Also maximum deviation, which was about 15.0% between the experiment measurement and simulation results, has come out at 90˚ bending. The spring-back angle results of 2.0 mm wall thickness show that spring-back distribution is close to linear.

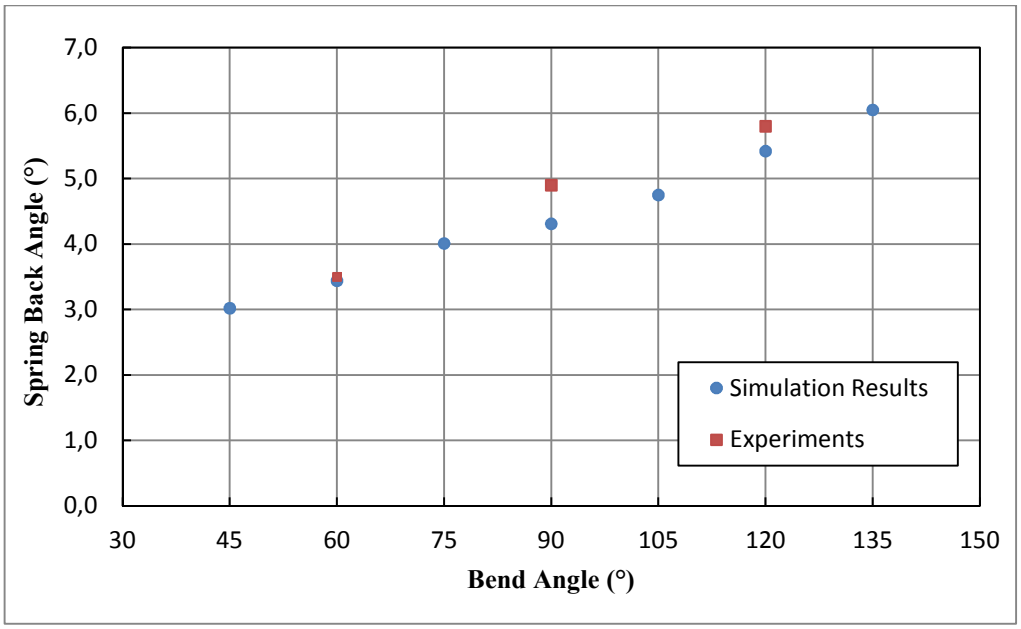

Figure 5-38 Spring-back Angle vs Bend Angle for SS304 Tubes having 1.5 mm Wall Thicknesses

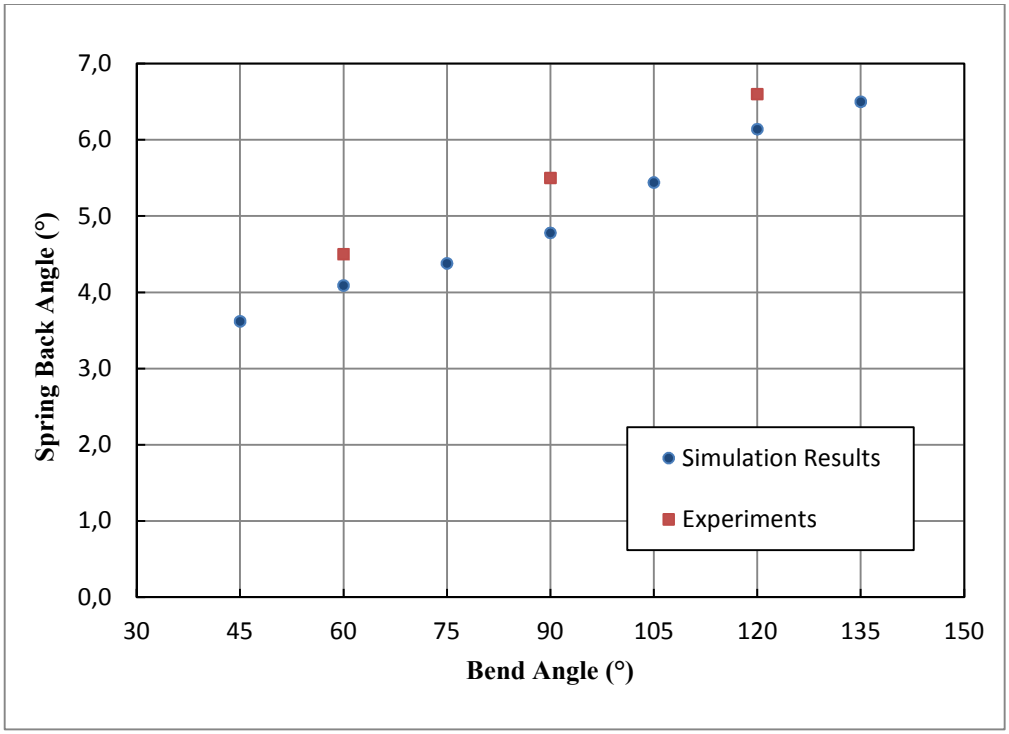

Figure 5-39 Spring-back Angle vs Bend Angle for SS304 Tubes having 2.0 mm Wall Thicknesses

5.3.4.4 Comparison of Spring-back Angles

All spring-back angle results for SS304 tubes are presented in Figure 5-40 which illustrates that as the tube wall thicknesses increase, spring-back angles increase as well. Both experimental and simulation results have an increasing tendency with increasing tube wall thicknesses and also bend angles.

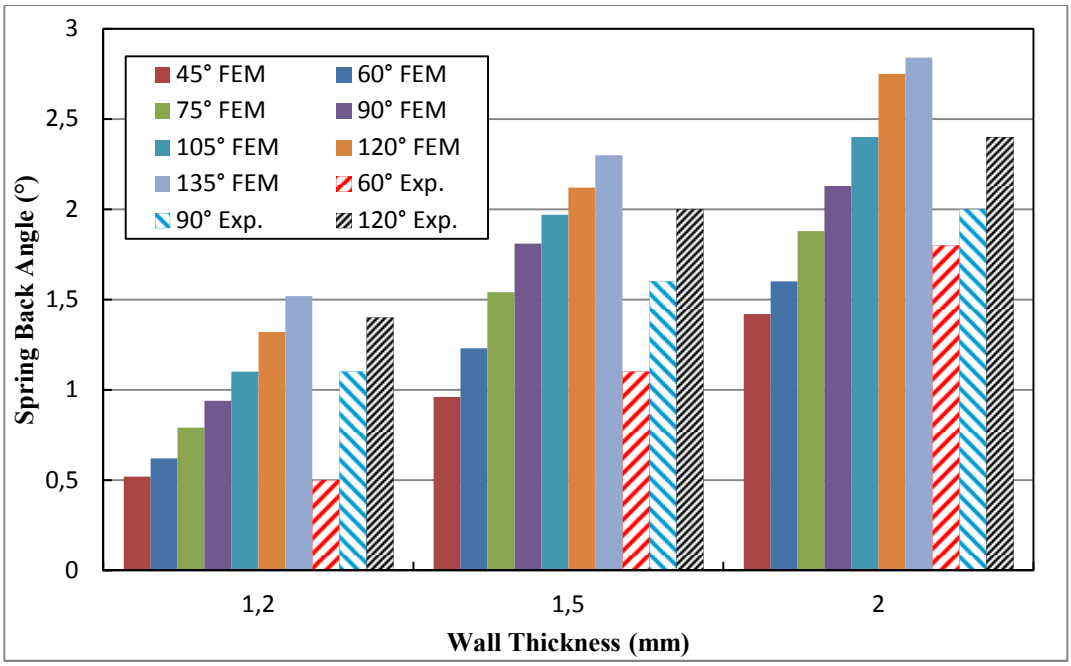

Figure 5-40 Wall Thickness vs Spring-back Angles for SS304 Tubes

CHAPTER 6

CONCLUSIONS

The main aim of the study is to investigate the characteristics of the rotary draw bending process. Variation of maximum stress and maximum strain values, variation of cross-section distortions, variation of wall thickness changes and variation of spring-back values with respect to bend angle and tube wall thicknesses are the main concern of the process. In this study, the tubes with two different materials; SS304 Stainless Steel and St37 Steel, with three different thicknesses; 1.2 mm, 1.5 mm and 2 mm, are used in the finite element simulations and tube bending experiments. Results are obtained by using different bend angles between 45° and 135° with the increment of 15°.

6.1 Conclusions

- The position of the tube seam does not have a significant effect on spring-back angles. However, cross-section distortions and wall thickness changes are dependent on the seam position. Considering the results obtained by the bending experiments, tube seams should be placed at the upper or lower side of the tube but not at the extrados or the intrados.

- The outer side of the bent tubes undergoes tension and the inner side undergoes compression. Hence the outer side of the tube gets thinner and the inner side of the tube gets thicker as it is expected. It is observed that, the percentage of the thickening at the intrados is larger than the percentage of the thinning at the extrados under the same conditions.

- Maximum stress and maximum strain occurred at extrados of the tubes and results showed that, with the increasing tube wall thicknesses maximum strain and stress values decrease. St37 tubes undergo higher strains when compared to SS304 ones.

- It is observed that, spring-back angle values increase almost linearly with increasing bend angle. SS304 Stainless Steel tubes have larger spring-back angles compared to the St37 Steel tubes at the same conditions due to their elastic properties since higher modulus of elasticity of the tube material results in higher spring-back angle values. Results illustrated that, spring-back amounts increase with increasing tube wall thicknesses.

- The wall thickness change results showed that, wall thickness changes increase with increasing bend angle. Also they decrease with increasing tube wall thicknesses. Since the SS304 material is stronger than St37, SS304 tubes had less wall thickness changes compared to St37 ones.

- Ovality values increase with increasing bend angle whereas they decrease with increasing tube wall thicknesses which imply that thicker tubes undergo less cross-section distortion. St37 tubes had higher cross-section distortions than SS304 ones.

- SS304 tubes have higher spring-back angles but they have less cross-section distortion compared to St37 ones. It means, in rotary draw bending process material selection should be done properly to obtain the desired bending characteristics.

When all the results are considered, it can be said that, the finite element simulation results that are obtained by using a commercial explicit dynamic solver are in good agreement with the experimental results achieved by using a rotary draw bending machine.

6.2 Future Work

Since the results presented in this thesis are valid for the materials and geometries used, for future work, in order to obtain the detailed characteristics of the rotary draw bending process, more bending experiments and simulations should be performed for different materials, bend angles and dies. Also, since the process is highly dependent on the ability of the bending machine, more precise, well controlled bending machines would be useful to minimize the deviations between the finite element and experimental results. Since the variation of the wall thicknesses affect the results, tubes having more precise dimensions can be used. Accurate modeling of the friction but not assuming the friction coefficients would also decrease the error. Furthermore, utilization of a more precise angle measuring device can be helpful. This study can be extended to be used in different tooling geometries to consider a wide range of tube bending processes.

REFERENCES

1. Powell, G.; Avitzur, B.: Proceedings of the North American Metalworking Research Conference, USA, (1972), pp. 63–83.

2. Stelson, K.A.; Lou, H.: Three Dimensional Tube Geometry Control for Rotary Draw Tube Bending Part1: Bend Angle and Overall Tube Geometry, Journal of Manufacturing Science and Engineering, 123 (2002), pp. 258-265.

3. Zhang, Y.; Redekop, D.: "Shell element simulation of the push method of tube bending", Department of Mechanical Engineering, University of Ottawa, Ottawa, Canada, (2006).

4. Lundqvist, J.: "Numerical Simulation o Tube Hydroforming, Adaptive Loading Parts", Luleal University of Technology, Sweden, (2004).

5. Ahmetoglu, M.; Altan, T.: "Tube hydroforming: State-of-the-art and Future Trends", Journal of Materials Processing Technology, 98 (2000), pp. 25-33.

6. Zeng, J.; Liu, Z.; Champliaud, H.: "FEM dynamic simulation and analysis of the roll-bending process for Forming a Conical Tube", Journal of Materials Processing Technology, 198 (2008), pp.330–343.

7. Hagenah, H.; Vipavc, D.; Plettke, R.; Merklein, M.: "Numerical Model of Tube Freeform Bending by Three-Roll-Push-Bending", 2nd International Conference on Engineering Optimization September 6 - 9, (2010), pp. 1-3.

8. Plettke, R.; Vatter, P.H.; Vipave, D.; Cojutti, M.; Hagenah, H.: "Investigation on the Process Parameters and Process Window of Three-Roll-Push-Bending", pp. 1662 – 36th MATADOR Conference.

9. Miller, J.E.; Kyriakides, S.; Bastard, A.H.: "On Bend-Stretch Forming of Aluminum Extruded Tubes - I: Experiments", International Journal of Mechanical Sciences, 43 (2001), pp. 1283-1317.

10. Miller, J.E.; Kyriakides, S.; Bastard, A.H.: "On Bend-Stretch Forming of Aluminum Extruded Tubes - II: Analysis," International Journal of Mechanical Sciences, 43 (2001), pp. 1319-1338.

11. Clausen, A.H.; Hopperstad, O.S.; Langseth, M.: "Stretch Bending of Aluminium Extrusions for Car Bumpers", International Journal of Mechanical Sciences, 43 (2001), pp. 3-12.

12. Wang, J.; Verma, S.; Alexander, R.; Gau, J.T.: "Springback Control of Sheet Metal Air Bending Process", Journal of Manufacturing Processes, 10 (2008), pp. 21-27.

13. Garcia-Romeu, M.L.; Ciurana, J.; Ferrer, I.: "Springback Determination of Sheet Metals in an Air Bending Process Based on an Experimental Work", Journal of Materials Processing Technology, 191 (2007), pp. 174–177.

14. Zhao, G.Y; Liu Y.L; Yang, H.; Lu C.H.: “Cross-sectional Distortion Behaviors of Thin-walled Rectangular Tube in Rotary-draw Bending Process”, Transactions of Non-ferrous Metals Society of China, 20 (2010), pp. 484-489.

15. Yang, H.; Lin, Y.: “Wrinkling Analysis for Forming Limit of Tube Bending Processes”, Journal of Materials Processing Technology, 152 (2004), pp. 363–369.

16. Li, H.; Yang, H.; Zhan, M.; Gu, R.J.: “A new method to accurately obtain wrinkling limit diagram in NC bending process of thin-walled tube with large diameter under different loading paths”, Journal of Materials Processing Technology, 177 (2006), pp.192–196.

17. Li, H.; Yang, H.; Song, F.F.; Zhan, M.; Li, G.J.: “Springback Characterization and Behaviors of High-strength Ti-3Al-2.5V Tube in Cold Rotary Draw Bending”, Journal of Materials Processing Technology, Accepted Manuscript, (2012).

18. Zhan, M.; Yang, H.; Huang, L.: “A Numerical-analytic Method for Quickly Predicting Springback of Numerical Control Bending of Thin-walled Tube”, J. Mater. Sci. Technol., (2006), Vol.22 No.5.

19. Li, C.; Yang, H.; Zhan, M.; Xu, X.D.; Li, G.J.: “Effects of Process Parameters on Numerical Control Bending Process for Large Diameter Thin-Walled Aluminum Alloy Tubes”, Transactions of Non-ferrous Metals Society of China, 19 (2009), pp. 668-673.

20. Mentella, A.; Strano, M.: “Rotary Draw Bending of Small Diameter Copper Tubes: Predicting the Quality of the Cross-section”, Proceedings of the Institution of Mechanical Engineers, Part B: Journal of Engineering Manufacture, October 2011, pp. 274.

21. Tang, N.C.: “Plastic-deformation Analysis in Tube Bending”, International Journal of Pressure Vessels and Piping, 77 (2000).

22. Wang, J.; Agarwal, R.: Tube Bending Under Axial Force and Internal Pressure, Journal of Manufacturing Science and Engineering, 128 (2006), pp. 598-605.

23. Penekli, U.: “Finite Element Anaylsis o Bending Operation of Aliminum Profiles”, M.s Thesis, Middle East Technical University, April 2008.

24. Chunfeng, L.; Yuying, Y.; Guofeng, G.; Weili, X.; Junting, L.: “Research on the section distortion of hat-section profiles in rotary draw bending with stretching force”, Journal of Materials Processing Technology, 94 (1999).

25. Zhao, G.Y.; Liu, Y.L.; Yang, H.; Lu, C.H.; Gu, R.J.: “Three-dimensional finite elements modeling and simulation of rotary-draw bending process for thin-walled rectangular tube”, Materials Science and Engineering A, 499 (2009), pp. 257–261.

26. Li, H.; Yang, H.; Zhan, M.; Kou, Y.L.: “Deformation behaviors of thin-walled tube in rotary draw bending under push assistant loading conditions”, Journal of Materials Processing Technology 210 (2010) pp.143–158.

27. Yang, J.B.; John, B.H.; Oh, S.I.: “The Tube Bending Technology of a Hydroforming Process for an Automotive Part”, Journal of Materials Processing Technology, 111 (2001), pp. 175-181.

28. Bhatti, M.A.: Advanced topics in Finite Element Analysis of Structures, (2006).

29. Anza, J.J.; Gutierrez, M.A.: “Metal forming simulation: Numerical efficiency in rolling processes - part I”, Engineering Computations, (1998), Vol. 15, Iss: 8, pp. 1049 – 1072.

30. ANSYS LS-DYNA User’s Guide, Ansys Inc. Southpointe 275 Technology Drive Canonsburg, PA 15317, April 2009.

31. LS-DYNA Theoretical Manuel, Livermore Sotware Technology Corporation, May 1998.

32. Kutt, L.M.; Pifko, A.B.; Nardiello, J.A.; Papazian, J.M.: “Slow-dynamic Finite Element Simulation of Manuacturing Processes”, 12th U.S. National Congress of Applied Mechanics, Seattle, WA, 26 June-l July, (1994).

33. Dynaform Material Library

34. ANSYS 11.0, Documentation for ANSYS, Chapter 2.4. 2007.

APPENDIX A

CODES FOR PREPARING FINITE ELEMENT MODEL

In this appendix, APDL [34] (ANSYS Parametric Design Language) codes are given for St37 Steel Tube having wall thickness of 2 mm, bending angle of 90º and bend radius of 62.5 mm. The code is a sample and not fully detailed.

Table A-1: Finite Element Model for St37 Tube, R=125 mm and t=2 mm

/BATCH
/COM,ANSYS RELEASE 11.0
/input,menust,tmp,'',,,,,,,,,,,,,,,1
/GRA,POWER
/GST,ON
/PLO,INFO,3
/GRO,CURL,ON
/CPLANE,1
/REPLOT,RESIZE
WPSTYLE,,,,,,,,0
/REPLOT,RESIZE
/COM,ANSYS RELEASE 11.0
/input,menust,tmp,'',,,,,,,,,,,,,,,1
/GRA,POWER
/GST,ON
/PLO,INFO,3
/GRO,CURL,ON
KEYW,PR_SET,1
KEYW,PR_STRUC,1
KEYW,LSDYNA,1
/PREP7

!*Element types
ET,1,SHELL163
ET,2,SHELL163
ET,3,SHELL163
*SET,_RC_SET,1,
R,1
!*THİCKNESS 2
RMODIF,1,1, ,5,2, , , ,
*SET,_RC_SET,2,
R,2
RMODIF,2,1, , ,2, , , ,
*SET,_RC_SET,3,
R,3
RMODIF,3,1, , ,2, , , ,
!*1.material
MAT,1,
MP,DENS,1,7.85E-09
MP,EX,1,2.07E+05
MP,NUXY,1,0.28
TB,PLAW,1,,,2,
TBDAT,1,**
TBDAT,2,**

Table A.1 Continued

TBDAT,3,*
TBDAT,4,0
TBDAT,5,0
TBDAT,6,*
!*2.material
EDMP,RIGI,2,7,4
MP,DENS,2,7.85e-9
MP,EX,2,2e5
MP,NUXY,2,.3
!*3.materil
EDMP,RIGI,3,7,7
MP,DENS,3,7.85E-009
MP,EX,3,2E+005
MP,NUXY,3,0.3
!*MODELLING
WPSTYLE,,,,,,,,1
wpro,,,90.000000
!*Rotary bend die
CYL4, ,62.5,13.5
K,5,,,,
K,6,,,219.3,
AROTAT,3,4,,, , ,5,6,90, ,
K,11,140,,,
LSTR,5,11
ADRAG,1,2,3,4,,,10,,,,,
ADELE,1, , ,1
!*pipe
K, ,-300,,,
K, ,100,,,
LSTR, 15, 16
wpoff,0,0,-290

wpoff,0,0,290
!*Pressure die
CYL4, ,62.5,13.5
K,29,-230,0,0
LSTR,5,29
ADRAG,32,33,,,,,36,,,,,
ADELE, 1, , ,1
!*grouping
ASEL,S,, ,8,9
ASEL,A, , ,10,11
CM,pipe,AREA
ALLSEL,ALL
CMSEL,U,PIPE
ALLSEL,BELOW,AREA
ASEL,S,, ,2,3
ASEL,A, , ,4,5
ASEL,A, , ,6,7
CM,rot_die,AREA
CMSEL,U,rot_die
ALLSEL,BELOW,AREA
ASEL,S,, ,12,13
ASEL,A, , ,13,15
CM,sta_die,AREA
ALLSEL,ALL
!*MESH
CMSEL,S,PIPE
AATT, 1, 1, 1, 0,
AESIZE,PIPE,4,
MSHAPE,0,2D
MSHKEY,1

Table A.1 Continued

CYL4, ,62.5,11.5
ADRAG,20,21,22,23,,,19,,,,,
ADELE, 1, , ,1
AESIZE,rot_die,8,
AATT, 2, 2, 2, 0,
MSHAPE,0,2D
MSHKEY,1
AMESH,rot_die
ALLSEL,ALL
CMSEL,S,sta_die
AATT, 3, 3, 3, 0,
AESIZE,PIPE,6,
MSHAPE,0,2D
MSHKEY,1
AMESH,sta_die
ALLSEL,ALL
!*SOLU
*DIM,time,ARRAY,2,1,1, , ,
*SET,TIME(2,1,1) , 0.0201
*DIM,rotation,ARRAY,2,1,1, , ,
*SET,rotation(2,1,1) , -1.5714
!*create parts
EDPART,CREATE
!*contact (Automatic Single Surface Contact)
EDCGEN,ASSC, , ,0.1,0.1,0,0,0, , , , ,0,10000000,0,0
!*Load
EDLOAD,ADD,RBRZ,0,2,TIME,rotation, 0, , , , ,
!*die inertia
*DIM,inertia, ,6

AMESH,PIPE
ALLSEL,ALL
CMSEL,S,rot_die
ALLSEL,BELOW,AREA
CM,force,NODE
*DIM,force,ARRAY,2,1,1, , ,
*SET,FORCE(2,1,1) , -10000
EDLOAD,ADD,FY,0,FORCE,TIME,FORCE, 0, , , , ,
ALLSEL,ALL
/SOL
TIME,0.02,
EDOPT,ADD,blank,BOTH
EDWRITE,BOTH,'R62.5_t2','k',' '
solve
SAVE
!*Spring back!
FINISH
/FILNAME,samplespring-back_implicit,0
/PREP7
ETCHG,ETI
SHPP,OFF
UPGEOM
tbdele, all, all
UPGEOM,1,LAST,LAST,'**','rst',' '
eplot
esel, s, mat, , 1
nsle
eplot
D,P51X, , , , , ,ALL, , , , ,

Table A.1 Continued

*SET,inertia(1),44.26,4.95,0,43.6,0,73.0
EDIPART,2,ADD, ,2.087e-3,0,inertia
FLST,5,2,5,ORDE,2
FITEM,5,16
FITEM,5,-17
ASEL,S, , ,P51X
RIMPORT,DYNA,STRESS,ELEM,LAST,LAST,'**','rst',' ', , ,
PLNSOL, U,SUM, 1,1.0

APPENDIX B

CASE STUDY: OBTAINING A BENT TUBE HAVING 90° FINAL TUBE ANGLE

In the experiments bending angles were selected as 60˚, 90˚ and 120˚. However, because of the spring-back, the final tube angles has come out to be smaller than those values. As a simple solution, to compansate the spring-back, overbending actions are performed in industry. Therefore, as a final touch of the thesis, a bending experiment with finite element simulations were made with the need of a final tube angle of 90˚. A SS304 Stainless Steel tube with a wall thickness of 1.5 mm is used for this purpose, all other bending parameters were kept same with the ones presented in the thesis.

An iterative solution with the constructed finite element model is accomplished. The aim is to find the initial tube bending angle to obtain a final tube angle of 90˚. After many iterations, initial bending angle is found as 95.1˚. Then, a bending experiment with that initial angle is carried out and final tube angle is measured. In Figure C-1 bent tube is shown, to measure the final tube angle, tangent plates are used.

Figure B-1 Tube Bending for the Case Study

In this case study, final tube angle came out as 90.6˚ with a 0.6˚ deviation from the target value.

APPENDIX C

ANGLE MEASURING DEVICE

Digital angle measuring device which was used in the experiments part is shown in Figure C-1.

Figure C-1 Digital Angle Measuring Device